Available online at www.sciencedirect.com

ScienceDirect

COORDINATION CHEMISTRY REVIEWS

Coordination Chemistry Reviews 251 (2007) 1259–1280

www.elsevier.com/locate/ccr

Review

A coordination chemistry approach towards ternary M/14/16 anions

Stefanie Dehnen*, Maike Melullis

Fachbereich Chemie, Philipps-Universität Marburg, Hans-Meerwein-Straße, D-35043 Marburg, Germany

Received 18 August 2006; accepted 11 November 2006
Available online 21 November 2006

Dedicated to Professor Günther Schmid on the occasion of his 70th birthday.

Contents

Abstract

The synthesis and exploration of heterobimetallic chalcogenide compounds has been studied intensely during the last decade. Besides the general interest in the exploration of novel synthetic pathways and the structural attraction of the target compounds, today's research activity concentrates on the development of novel materials. Ternary chalcogenides as well as their molecular, nanostructured or mesostructured derivatives can be formally viewed as combinations of binary chalcogenometallates; accordingly, they provide combinations or mixtures of the specific properties, e.g. opto-electronics or magnetism of the formally underlying parent compounds. Despite the fact that many tetrel chalcogenides exhibit (photo-) semiconducting properties, only few reports were available on ternary M/14/16 aggregates; moreover, since the known M/14/16 complexes were usually generated from separate sources of the three components, it was practically impossible to design the size or structure of the 14/16 fragment which would control the spatial separation of the transition metal atoms. As an efficient alternative, we have developed a coordination chemical route by using a preformed binary 14/16 source: by reactions of *ortho*-chalcogenotetrelate anions $[E'E_4]^{4-}$ under ambient conditions in solution, we gain systematic access to complexes with definite, close proximity of the transition metal centers—allowing for interaction of the latter within

---

* Corresponding author. Tel.: +49 6421 282 5751; fax: +49 6421 282 5653.
E-mail address: dehnen@chemie.uni-marburg.de (S. Dehnen).

0010-8545/$ – see front matter
doi:10.1016/j.ccr.2006.11.003

the heterobimetallic molecular anions and anionic networks. This review will focus on synthesis, structures and physical properties of the resulting quaternary compounds with M/14/16 anions.

Keywords: Chalcogenotetrelates; Ternary anions; X-ray crystallography; Optical absorption; Magnetism

1. Introduction

1.1. Compounds with M/E′/E substructures

The stabilization of binary E/E′ aggregates of main group elements in the coordination sphere of transition metal ions M^{n+}, and thus the synthesis and exploration of ternary coordination compounds, has become an area of increasing research activity during the last decade. These investigations might be viewed as a modification and extension of the more established studies of transition metal complexes bearing homo-atomic polyanions of main group elements of Groups 14 [1], 15 [2] or 16 [3] as ligands.[1]

Most reports in this area focus on complexes of the general type $[M_xE'_yE_z]^q$ (*q*: charge, compensated by counterions or ligands) where chalcogen atoms E bridge the two types of (semi-) metal atoms E′ and M [4–6]. In these species, rather ionic M–E bonds exist besides rather covalent E′–E bonds. This clearly distinguishes these systems from heterobimetallic chalcogenide compounds with $[M_xM'_yE_z]^q$ fragments containing two different types of transition metal atoms M and M′ [7].

In addition to the general interest in the exploration of novel synthetic pathways and the structural attraction of the target compounds, recent work concentrates on the development of novel materials. In this regard, the study of the molecule to solid state transition by synthesis of nanostructured or mesostructured compounds, which is very popular for *binary* metal chalcogenides due to their interesting physical properties [8,9], is extended by the investigation of *ternary* metal chalcogenides or chalcogenometallates (the heavier homologues of oxosilicate anions): the latter can be viewed as a formal combination of two binary components; as a result, combination or mixture of the specific properties, e.g. the opto-electronics [10], might be observed, which is illustrated by comparison of band gaps of binary and ternary chalcogenides (Table 1). The same should be expected for an analogous elemental combination in compounds that are based on molecular, nanostructured or mesostructured species.

Despite the fact that many *tetrel* chalcogenides exhibit (photo-)semiconducting properties [12], only few reports were available, until the 1990s, on the synthesis and characterization of ternary M/14/16 complexes [4], whereas a large number of publications reported on the very much related area of compounds containing diverse M/15/16 substructures [5,6]. Most of the latter have been prepared by the employment of binary 15/16 reactants, e.g. the recently published $[(Cp^*Rh)_3Sb_2S_5]$ from $K_3[SbS_3]$ and $Cp^*_2Rh_2Cl_4$ [13], whereas in the case of the few compounds containing Group 14 atoms, the M/E′/E substructures have usually been generated providing separate sources for the transition metal, the tetrel and the chalcogen component, as for the ternary coordination polymers in $K_2[MnSnS_4]$ [14] or $K_2[MnSnSe_4]$ [15], which were synthesized by fusing Mn, Sn, K_2E, and E in the flux. This way, it was practically impossible to design the size or structure of the 14/16 fragment which would control the spatial separation of the transition metal atoms. One class of M/14/16 complexes was even synthesized by reactions of organometallic substituted tetrel complexes with chalcogen sources, which naturally determined the occurrence of M–E′ units and thereby excluded any M–E–E′ bridging. Examples are the reaction of $[\{Cp^*(CO)_2Mn\}_3(\mu_3\text{-}Sn)]$ with H_2S or $[\{Cp(CO)_2Fe\}SnCl_3]$ with Na_2Se to produce $[\{(Cp^*(CO)_2MnSn)_3S_4\}Mn(THF)_3]$ in the first case [16] or $[\{Cp(CO)_2Fe\}_3Sn_3Se_4Cl]$ in the latter [17].

1.2. From binary to ternary anions: coordination chemistry with chalcogenotetrelates

Subsequent to the early work by Bedard et al., who generated microporous A/M/E′/S solids by combining elemental

Table 1
Band gaps of several chalcogenides of electron-rich transition metals, main group elements or a combination of both [10–12]

	Band gap (eV)
Binary phase	
Cu_2S	1.1–1.3
Cu_2Se	0.9–1.1
Ag_2S	0.8–1.0
Ag_2Se	0.2
CdSe	1.7–2.3
In_2S_3	2.6
In_2Se_3	1.4
$GeSe_2$	2.5
$SnSe_2$	2.7
As_2S_3	2.6
Ternary phase	
$CuInS_2$	1.5
$CuInSe_2$	1.0
$CdIn_2Se_4$	1.4
Cu_2GeSe_3	0.9
Ag_8GeSe_6	0.9
Ag_8SnSe_6	0.8
$AgAsS_2$	2.0

---

[1] Unless specified, M or M′ will denote transition metal atoms, E′ represents atoms of Groups 13–15 (triels, tetrels, pnicogens) and E replaces chalcogen atoms S, Se, or Te.

M and $E'S_2$ in the presence of organic templates [18a], the transfer of chalcogenotetrelate anions or their derivatives into the coordination sphere of transition metal centers was first reported in 1994 by three independent groups: Yaghi et al. prepared the first crystallographically determined example of $A_2[ME'_4E_{10}]$ open framework compounds (A = alkali metal or ammonium cation) employing a preformed E'/E aggregate: crystalline $(NMe_4)_2[MnGe_4S_{10}]$ was obtained by reacting aqueous solutions of $(NMe_4)_4[Ge_4S_{10}]$ and $Mn(OAc)_2·4H_2O$ [18b]. Okazaki and co-workers used the organic substituted (tetrachalcogeno)stannates $Tb(Tip)Sn(S_4)$ or $Tb(Tip)Sn(Se_4)$, and the related $Tb(Tip)Sn(SH)_2$ for reactions with various transition metal carbonyl complexes at 70–120 °C in toluene to obtain complexes like $Tb(Tip)SnS_2Ru_2(CO)_6$ [19]. Dhingra and Haushalter described synthesis and structure of $K_2[HgSnTe_4]$ by solvothermal reaction of $K_4[SnTe_4]$ with $HgCl_2$ in 1,2-diaminoethane (*en*) [20]. In spite of these promising entries, the "14/16 + M" routes were not extended during the following years apart from the synthesis of some further variations of $A_2[ME'_4E_{10}]$ phases ($A = NMe_4$; $M = Cu_2$, Ag_2, Mn, Fe; $E' = Ge$, $E = S$, Se) in a microcrystalline form [21,22]. A different goal has finally led to a renaissance of the coordination chemistry with chalcogenotetrelate anions: the presence of cetyltrialkylammonium ions (CTA) or cetylpyridinium ions (CP) led to the formation of mesostructured, ternary anionic frameworks $[M_xE'_yE_z]^{q-}$. These phases, e.g. $(CP)_3[Fe_4S_4Ge_4Se_{10}]$ [23] or $(CP)_2[PtSn_2Se_6]$ [24], represent a class of compounds with exciting opto-electronic properties, such as relatively narrow band gaps or intense photoluminescence; therefore, they are discussed as a novel type of non-oxidic zeolite-type materials. However, none of these complex compounds has been structurally determined until now, since they are not obtained as single crystals of an appropriate size, but rather precipitate as powders or microcrystals. Therefore, the proposed conservation of the $[E'_yE_z]^{q-}$ anions and the suggested structures are essentially based on elemental analyses and, in some cases, result from EXAFS analyses. Nevertheless, the opto-electronics and successful ion exchange experiments of such phases point at possible applications and confirm the synthetic potential of the reactants.

Our aim in this context has been to study the reaction behavior of chalcogenotetrelate anions in the presence of transition metal ions in solution at ambient temperatures. Before we started our investigations, only one type of reaction had been reported to be successful under these conditions, namely the above mentioned synthesis of $(NMe_4)_2[MnGe_4S_{10}]$ and related phases using $[Ge_4E_{10}]^{4-}$ anions ($E = S$, Se); unlike this, we were interested in the largely unknown reactivity and stability of *ortho*-chalcogenotetrelate anions $[E'E_4]^{4-}$, which represent the smallest and most sensitive 14/16 anions. Using these, we intended to gain access to complexes with closer proximity of the transition metal centers, which might then interact within the heterobimetallic, anionic networks. Moreover, we hoped to synthesize first compounds with molecular M/14/16 anions that might be of interest for both homogeneous catalytic applications and further chemical reactivity due to better solubility.

2. Experimental

2.1. The reactants: syntheses and characterization of ortho-chalcogenotetrelate salts

The synthesis and characterization of chalcogenotetrelate salts $A_x[E'_yE_z]$ (A = alkali metal or alkaline earth metal) has been explored for about three decades. Numerous working groups have studied these compounds for different purposes. According to the diverse activities in this field, different synthetic approaches were realized toward salts of binary 14/16 anions. The most common preparation pathway is still the fusion of the elements A, E' and E (Scheme 1) [25a] or reaction of binary chalcogenides A_xE with E' and E (Scheme 2) at high temperatures, in polychalcogenide fluxes or under solvothermal conditions [25b–g]. Purification of amorphous or microcrystalline products may be achieved by the ensuing extraction of the phases with polar solvents, like H_2O, alcohols or *en*, yielding respective solvates, like $[Ba_2(H_2O)_9][GeSe_4]$ (Fig. 1, top) [26], after evaporation or layering. If following a two-step fusion/extraction route, the products can be obtained in high yield as single crystals within one day (Scheme 3) [27].

Moreover, there exist synthesis routes in solution that equally allow for the isolation of very pure, crystalline chalcogenotetrelate salts in good yields. Krebs and coworkers, for instance, combined aqueous solutions of A_2E and freshly prepared $E'E_2$ to obtain salts such as $[Na_4(H_2O)_{16}][GeSe_4]$ [28a] or $[Na_4(H_2O)_{16}][SnSe_4]$ [28b] after slow evaporation of the mother liquor (Scheme 4). However, this route requires the solubility and stability of the alkali or alkaline earth metal chalcogenide in solution; this also holds for the second route in solution: as outlined in Scheme 5, reaction of A_xE with $E'Cl_4$ in water with ensuing layering by an organic solvent like acetone or THF is applicable for the synthesis of chalcogenotetrelates like $[Na_4(H_2O)_{14}][SnS_4]$ (Fig. 1, bottom) [28c,d].

2.2. The products: reactions of ortho-chalcogenotetrelates with transition metal compounds

The application of inorganic chalcogenotetrelate salts for the synthesis of compounds with ternary M/14/16 anions, thus the coordination chemical approach into this class of compounds, has been realized, so far, in two different ways. Whereas the pioneering work by Dhingra and Haushalter followed the solvothermal route [20], our approach, working in ROH solu-

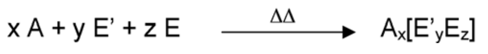

$$x\,A + y\,E' + z\,E \xrightarrow{\Delta\Delta} A_x[E'_yE_z]$$

Scheme 1. Synthesis of chalcogenotetrelate salts by fusion of elemental alkali(ne earth) metal, tetrel and chalcogen at high temperature [25a].

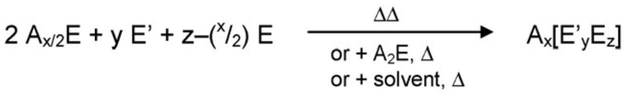

$$2\,A_{x/2}E + y\,E' + z-(^x/_2)\,E \xrightarrow[\text{or + solvent, }\Delta]{\Delta\Delta \quad \text{or + }A_2E,\ \Delta} A_x[E'_yE_z]$$

Scheme 2. Synthesis of chalcogenotetrelate salts by reaction of alkali(ne earth) metal chalcogenides, tetrel and chalcogen at high temperature [25b–g].

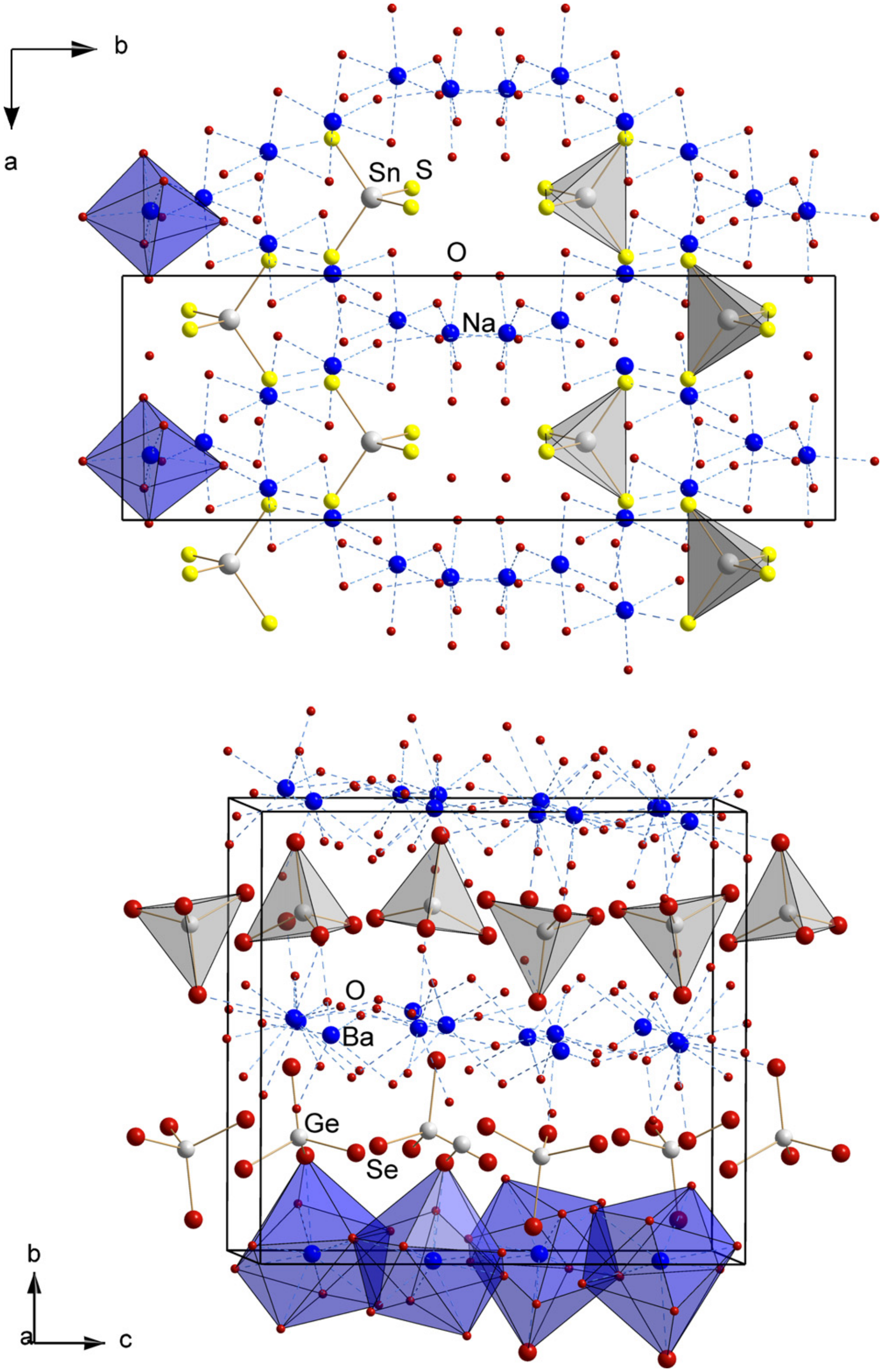

Fig. 1. Crystal packing diagrams of the alkaline earth selenogermanate salt $[Ba_2(H_2O)_9][GeSe_4]$ (top) [26] and the alkali metal thiostannate salt $[Na_4(H_2O)_{14}][SnS_4]$ (bottom) [28c,d].

$$6\,\mathrm{A} + 6\,\mathrm{Sn} \xrightarrow{\Delta\Delta} 6\,\mathrm{ASn} \xrightarrow[-\,4\,\mathrm{Sn}]{+\,6\,\mathrm{E},\ \Delta\Delta} \mathrm{A}_6[\mathrm{Sn}_2\mathrm{E}_6] \xrightarrow[-\,0.5\,\mathrm{Sn}]{+\,\mathrm{ROH}} 1.5\,[\mathrm{A}_4(\mathrm{H_2O})_n][\mathrm{SnE}_4]$$

Scheme 3. Synthesis of chalcogenostannate salts by a two-step reaction at high temperature *via* a binary A/Sn alloy, with ensuing extraction [26,27].

$$2\ Na_2E + E'E_2 \xrightarrow[2)\ -H_2O\ (evap.)]{1)\ aqua} [Na_4(H_2O)_n][E'E_4]$$

Scheme 4. Synthesis of chalcogenotetrelate salts by combining A_2E and freshly prepared $E'E_2$ in aqueous solution [28a,b].

$$4\ A_xE + E'Cl_4 \xrightarrow[2)\ +\ org.\ solvent]{1)\ aqua} [A_{2x}(H_2O)_n][E'E_4] + 2x\ A^{(2/x)+}_{aq} + 4\ Cl^-_{aq}$$

Scheme 5. Synthesis of chalcogenotetrelate salts by reaction of A_xE with $E'Cl_4$ in aqueous solution [28c,d].

tion (R = H, Me), has extended the early work by the Yaghi group [18]. Scheme 6 (preparation in solution) and Scheme 7 (synthesis *via* the solvothermal method) summarize all compounds with ternary, anionic M/14/16 substructures that have been structurally characterized so far.

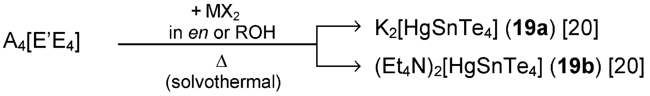

Scheme 7. Compounds synthesized by the solvothermal reaction of chalcogenotetrelate salts with transition metal chlorides in supercritical *en* or ROH (R = H, Me).

In the following discussion, the anionic substructures are assigned to different types (roman numbers **i**–**ix**). Compounds that were prepared by coordination chemical synthesis are given Arabic numerals **1**–**27**, employing the same number for isotypic salts. Phases containing isostructural or very much related anions that have, however, been generated by different synthetic pathways are indicated by roman numbers **I**–**IX**.

As a different but related alternative, Scheme 8 sketches reactions of chalcogenotetrelate salts with transition metal ions in the

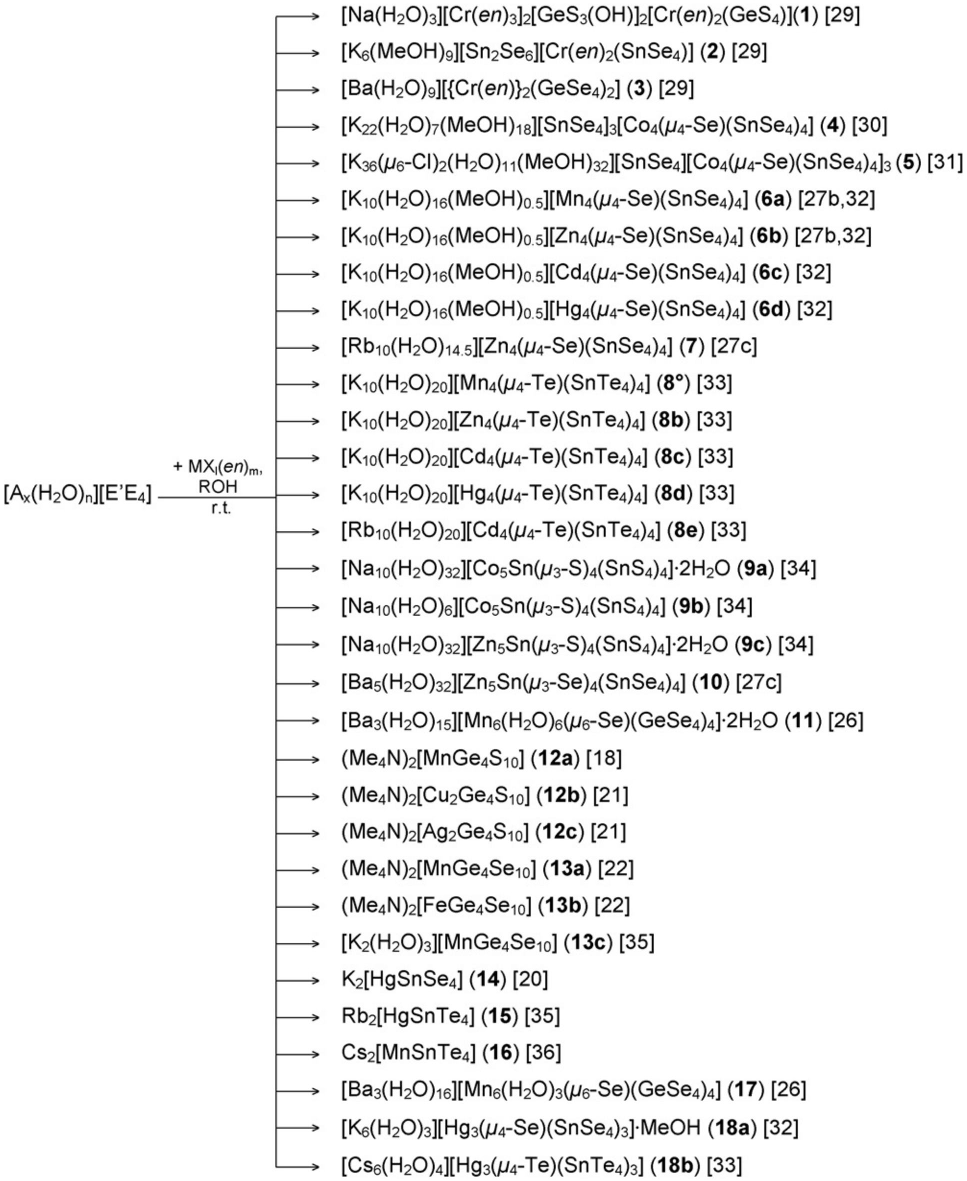

Scheme 6. Overview of compounds synthesized by reaction of chalcogenotetrelate salts with transition metal (pseudo)halogenides or *en* complexes (*en* = 1,2-diaminoethane) in ROH solutions (R = H, Me) at room temperature.

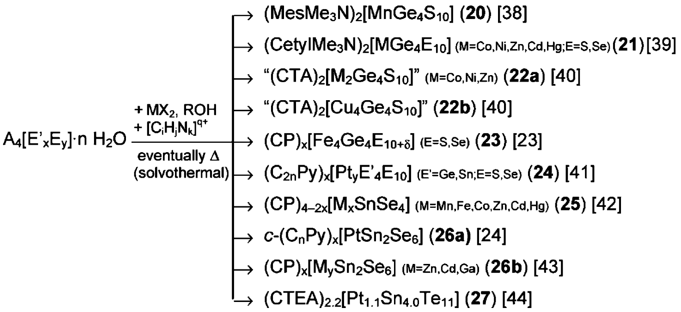

Scheme 8. Mesoporous compounds synthesized by reaction of chalcogenotetrelate salts with transition metal chlorides in the presence of ammonium salts with large organic substituents. *Abbreviations*: Mes = 2,4,6-trimethylphenyl, Cetyl = hexadecyl, CTA = cetyl-trialkylammonium, CP = cetylpyridinium, C_{2n} Py = alkylpyridinium with alkyl = $C_{2n}H_{4n+1}$, CTEA = cetyl-triethylammonium.

presence of ammonium salts with large organic substituents. The structures of the resulting mesoporous phases have not been clarified by X-ray crystallography as outlined before. Although the properties of these phases will not be discussed herein into detail, since they are subject of a number of further reports [37a–d], a summary and a general specification of their preparation is given to complete this overview.

3. Results and discussion

The structurally determined compounds containing M/14/16 anions that have been reported to date (Schemes 5 and 6) are either phases with discrete anions or possess an extended anionic substructure. Quite often, the latter can be derived from discrete units; therefore, the crystal structures of the first group will be presented in the next paragraph, followed by the discussion of phases with one-dimensional, two-dimensional or three-dimensional M/14/16 anions.

3.1. *Crystal structures of compounds with molecular M/14/16 anions*

Five different types of molecular M/14/16 anions have been characterized to date. These contain one, two, four, five or six transition metal centers besides chalcogenotetrelate units, and are stabilized by different, sometimes very complex counterion aggregates. Some of the structural motifs have also been obtained by different synthesis routes, such as solvothermal reactions of the M, E′ and E elements with alkali metal carbonates, or by reactions in a polychalcogenide flux, which will be pointed out for the respective examples (roman numbers). However, the coordination chemical route is yet the only one to enable access to all of these discrete M/14/16 anions. Fig. 2 shows the molecular structures of anionic M/14/16 complexes with one or two transition metal atoms, considering compounds **1** and **3** as examples.

The smallest species (type **i**, compounds **1** and **2**; Fig. 2a) can be viewed as mononuclear chromium complexes that contain two chelating *en* ligands besides one chelating $[E'E_4]^{4-}$ group. Alternatively, one may describe these as heterobimetallic, dinuclear Cr/E′ complexes with coordinating *en* or E ligands and two E bridges. The first view is in agreement with the preparation and the formal $[E'E_4]^{4-}$ for *en* or Cl^- exchange; the latter underlines the mixed-metal character, which might be of interest for future catalytic application. Type **ii** (compound **3**; Fig. 2b) is very much related to the first; however, only one *en* ligand binds to each Cr^{3+} center here, whereas the other four coordination sites are occupied by Se ligands from $[GeSe_4]^{4-}$. The chalcogenotetrelate groups link two Cr ions by using Se atoms as both μ and μ_3 bridging ligands. Both of these anionic structures are unique for the elemental M/14/16 composition; however, there exist some topologically related heterometallic complexes. Examples for type **i** analogues have recently been prepared by the Bensch group under solvothermal conditions: in $[Cr(en)_2(SbS_3)]$ [45] and $[\{M(tren)\}_2(Sn_2S_6)]$ (*tren* = tris(2-aminoethyl)amine, M = Co, Ni) [46], thioantimonate or thiostannate units also

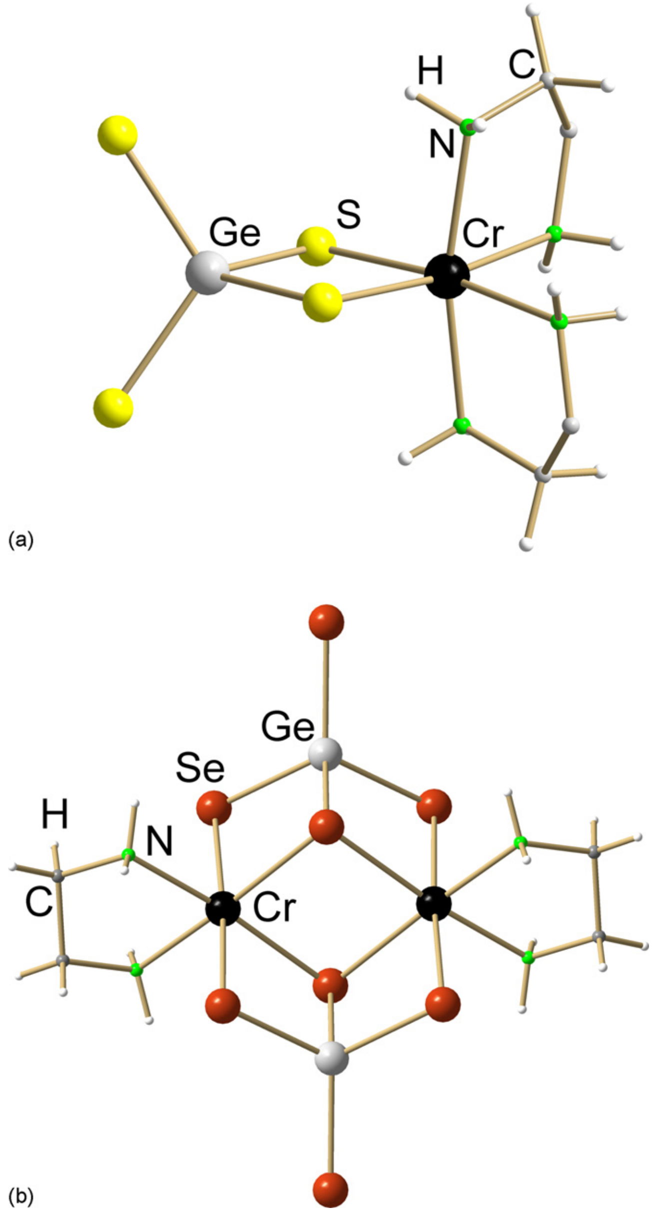

Fig. 2. Molecular structure of the anions of compounds **1** and **3** as examples for type **i** (a) and type **ii** (b) [29].

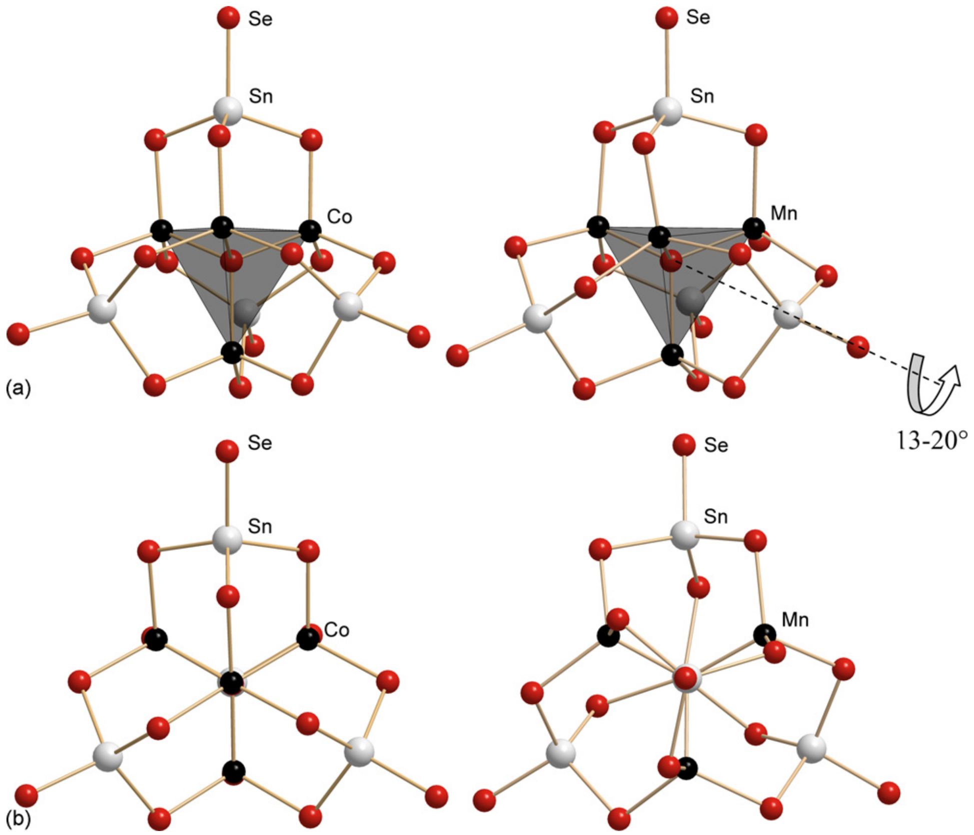

Fig. 3. P1-type super-tetrahedra (type **iii**): (a) C_3-symmetric anion in compound **4** (left hand side) [30] and the C_2-symmetric anion in compound **6a** (right hand side) [27b,32], illustrating the central [EM_4]-tetrahedra; (b) view along the threefold axis of the undistorted anion in **4** (left hand side) and the distorted anion in **6a** (right hand side).

act as chelating ligands by binding to an amine coordinated transition metal center *via* a chalcogen atom. The structure of the copper complex in $(HPnPr_3)_2[Cu_2Ga_4Cl_4Se_6(PnPr_3)_4]$, which was reported by Eichhöfer and co-workers [47], is similar to type **ii**. Here, tetrahedrally coordinated copper centers are linked by two corner-sharing $[Ga_2Se_4Cl_2]^{4-}$ units.

Type **iii** is the most common one until now. It occurs in compounds **4**–**8**, comprising numerous isotypic examples. In addition to the selenide and telluride compounds that were generated in our laboratory, diverse phases have been reported by Kanatzidis and co-workers containing M/14/S anions of this topology, namely $K_{10}[M_4(\mu_4\text{-}S)(SnS_4)_4]$ (**I**) (M = Fe: **Ia**, Co: **Ib**, Ni: **Ic**, Zn: **Id**, Mn: **Ie**, Cd: **If**, Hg: **Ig**) [48,49], $Cs_{10}[Cd(\mu_4\text{-}S)(SnS_4)_4]$ (**II**) [49] or $K_{10}[Zn(\mu_4\text{-}S)(GeS_4)_4]$ (**III**) [49], that were generated by combining M, Sn or Ge, K_2S or Cs_2S and S in the flux. This type of heterobimetallic complexes is presented in Fig. 3, exemplary for the C_3-symmetric cluster in **4** and the significantly distorted, C_2-symmetric species in **6a**.

This anion type represents a so-called P1 super-tetrahedron, which is the first member of the P*n* family of super-tetrahedral molecules. The P1 structure contains an inner tetrahedron $[A^1B^1_4]$, all faces of which are capped by (inverse) tetrahedra $[B^2A^2_4]$ under formation of ever three B^1–A^2 bonds (in the ternary anions, A^1 and A^2 represent the same, more electronegative element E, whereas B^1 and B^2 are (semi-)metal atoms M or E′, respectively). The fourth A^2 atom is terminal, representing one of the corners of the large tetrahedron that includes a total of *five* tetrahedra ("*Penta*-Tetrahedron", P*n*). This topology seems to exhibit an extraordinary stability, since it has been observed for a great number of diverse compounds [50]. The first report dates back 30 years, when von Schnering et al. described the carbosilane species $Si_8C_{17}H_{36}$ [51]. The same topology was found for numerous chalcogenide or pnicogenide bridged clusters of d^{10} metals Zn or Cd [52,53a–d], that were, however, wrapped by an organic ligand shell. The first purely inorganic compound featuring this structural motif – at the same time containing the first *ternary* P1 complex – was published by Eriksson et al. in 1990, who prepared the quaternary phase $Na_{10}[Be_4Si_4O_{17}]$ [54].

Very different counterions of counterion aggregates have been observed for the different variants of type **iii** compounds. These influence both crystal and molecular symmetry. Therefore, some of the clusters that have been observed possess perfect T_d symmetry [48,49], whereas several examples of lower symmetry down to C_1 were also reported. However, most anions are very close to the point group T_d, except those of compound **6** that show a more significant distortion (Fig. 3b): the four $[SnSe_4]^{4-}$ groups ($[B^2A^2_4]$ here) are rotated around the Se_t–Sn–(μ_4-Se) axes by 13–20° in the four phases, since all rotations follow the same rotational sense. Chiral molecules result (crystallographic C_2 symmetry). These compounds show the often found chirality of the crystal structures due both to the molecular symmetry and the crystal packing of ionic components and solvent molecules. However, the crucial influence of the counterion aggregates on the distortions of the anionic molecules was confirmed by means

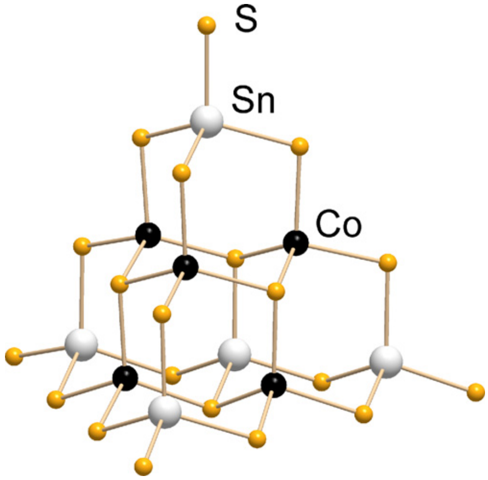

Fig. 4. T3-type super-tetrahedron (type **iv**) in compound **9a** [34].

of quantum chemical investigations of the isolated anionic clusters, which show convergence into completely undistorted anions for all systems calculated so far [32,34].

Complexes with five transition metal ions per anion are found in compounds **9** and **10** (type **iv**, Fig. 4); the anions represent so-called T3-type super-tetrahedra. This third member of the T*n* super-tetrahedra family, all of which accord to fractions of the sphalerite structure, is a very stable arrangement of 30 atoms as reflected by the large number of molecules with this topology [50].

However, the two variants of compound **9** and compound **10** are the only three known phases that comprise discrete T3 anions without an organic ligand shell; previously, the T3-type was observed with many binary, ligand clad chalcogenide or pnicogenide clusters of d^{10} transition metals Zn, Cd, or Hg, like $[Cd_{10}S_4(SPh)_{16}]^{4-}$ [52], $[Hg_{10}Te_4(SePh)_{12}(PPh\textit{n}Pr_2)_4]$ [55a,b], $[Zn_{10}Cl_{12}(PSiMe_3)_4(PEt_2Ph)_4]$ [56], with wrapped Zn/E or Cd/E nanoparticles [57] and with binary thio(semi)metalates of d^{10} main group elements B [58], Ga [59], In [60] or Sn [61]. Similar to **9** and **10**, the cited main group elemental thiolates do not exhibit a ligand shell, but neither do they represent discrete T*n* anions; they are rather linked to form a variety of interesting three-dimensional networks [50], e.g. by sharing the four corner S atoms of $[B_{10}S_{16}S_{4/2}]^{6-}$ with adjacent cluster fragments in $Ag_3B_5S_9$ [58]. The only further discrete example among the thiolates quoted is observed in $Na_8Sn_{10}O_4S_{20}\cdot 32H_2O$, however, representing a "stuffed" T3 super-tetrahedron with four additional O^{2-} ions in the tetrahedral holes of the cluster [61]. A ligand-clad, *ternary* M/13/16 cluster has been reported very recently with the compound $(AsPh_4)_2[Cu_6In_4(SePh)_{16}Cl_4]$ [62].

So far, the anions of compounds **9** and **10** represent the only – *i.e.* both the smallest and largest – examples of T*n*-type clusters that were observed with M/14/16 complexes. For the elemental combination M/13/16 or for binary anions there also exist larger T4 or T5 super-tetrahedra; examples are the T4 type anion $[Cd_4In_{16}S_{35}]^{14-}$ [63] or the T5 type anion $[Mn_{35}O_{56}]^{30-}$ [64]. In the majority of the compounds reported, such clusters are linked to form open framework structures as observed with the corner-linked T5-type super-tetrahedra in $(TMDPH_2)_{6.5}$ $[Cu_5In_{30}S_{54}]$ (TMDP = 4,4′-trimethylenedipiperidine, $C_{13}H_{26}N_2$) [65]. Moreover, defect variants with open centers have been described, as well as further structural variations (denoted as Cn or Cn, m type compounds), which represent composites of different cluster types [50].

All of the cited compounds containing M/13/16 anions – as well as the related binary 12/16 or 13/16 aggregates [50] – were obtained under solvothermal conditions from separate sources for the incorporated main group elemental atoms; the oxomanganate was prepared by a high temperature redox reaction from Mn, CdO, Na_2O, and $NaSO_4$ [64]. It is not clear yet, whether a solution approach generally excludes the controllable formation and crystallization of salts of larger and thus higher negatively charged anionic molecules;[2] however, since the participation of Group 14 atoms leads to a lower total charge than does the same amount of Group 13 elements in the cited compounds – given that both types of main group atoms occupy comparable positions in similar M/E′ ratios within the cluster ions – it is likely that an appropriate choice of both solvent and counterions might enable access to larger M/14/16 systems by a coordination chemical route, as well.

The fifth anionic structure, type **v**, is present in compound **11**, which is the third of the three alkaline earth (Ba^{2+}) salts of M/14/16 anions reported to date besides **3** and **10**. Type **v**, which is shown in Fig. 5, represents a hybrid between a super-octahedral cluster and a super-tetrahedron.

Six Mn centered $[MnSe_5O]$ octahedra share their faces to form a large octahedron with three atoms per edge—an atomic arrangement which is well known from the $[Mo_6O_{19}]^{2-}$ polymolybdate anion [66]. Additionally, four $[GeSe_4]^{4-}$ groups share four of the eight Se_3 central faces with the large octahedron, causing an overall (near) tetrahedral symmetry. This combination of octahedrally and tetrahedrally surrounded (semi-)metal centers is unique for M/14/16 anions; so far, only tetrahedral coordination for both transition metal atoms and Group 14 atoms has been described with these complexes. It is, however, surprising that this feature was not observed before, since the thermodynamically stable α-MnSe indeed crystallizes in the halite structure, bearing $[MnSe_6]$ octahedra, and since the structure of the very much related, ternary phase Mn_2GeSe_4 [67] also consists of $[MnSe_6]$ and $[GeSe_4]$ groups. Only one further cluster molecule has been reported so far with this topology: the heterobimetallic anion in $[Cu_4Nb_6Se_{12}O(PMe_3)_{10}][Cu_4NbSe_4Cl_2(PMe_3)_4]\cdot 1.5DMF$, [68] which shows, however, a different elemental composition and was prepared by reaction of $(Me_3Si)_2S$ with $[CuCl(PMe_3)_3]$ and $(NEt_4)_2[NbSe_3\text{-}(Se^tBu)]$ in DMF.

Comparing the overall composition of the members of each of these five groups of compounds, additionally considering

---

[2] We refer to the *total* charge; depending on the average charge of the M/E′ combination, the total charge increases up to a certain M/E′ to E ratio in spite of a decreasing (semi-)metal:chalcogen ratio at larger clusters. For T*n* type anions e.g., pure +III metal oxidation states lead to an increasing value of the anionic charge up to the T4 generation before decreasing; for +IV metal oxidation states, the reduction of total negative charge is observed upon T3.

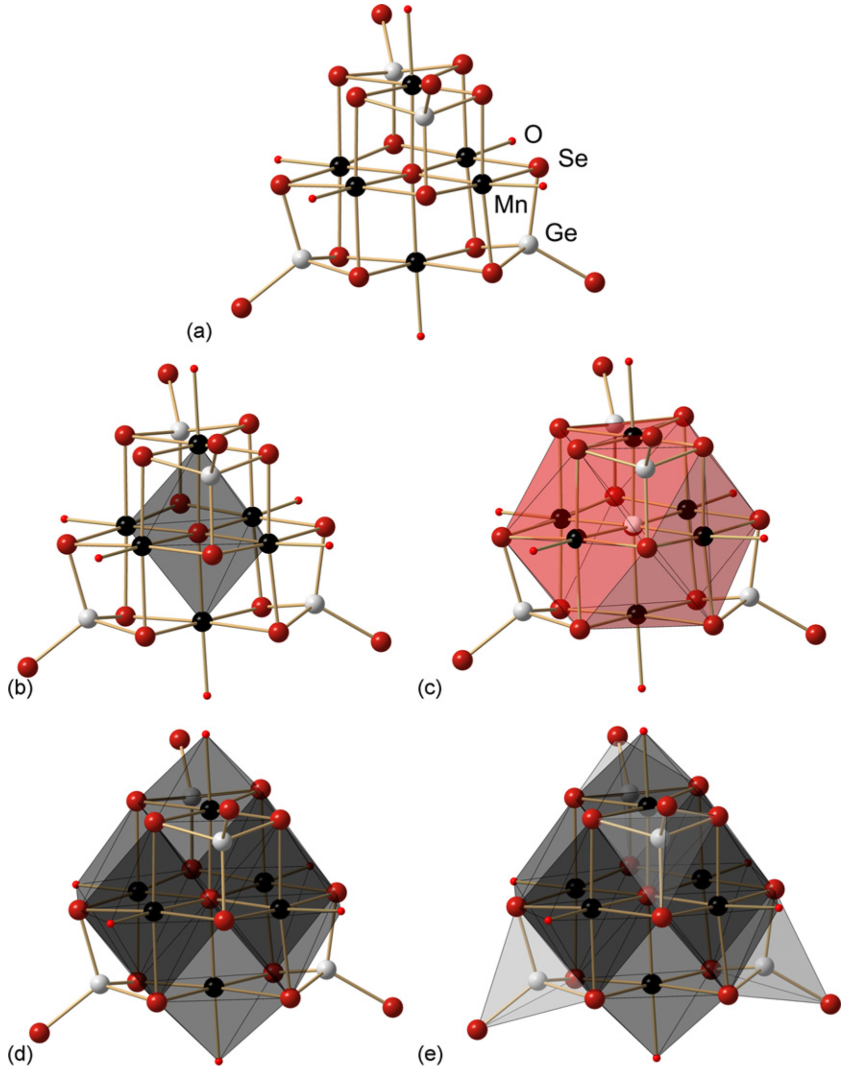

Fig. 5. Molecular structure of the H_2O-ligated, ternary Mn/Ge/Se anion in **11** (a) [26] and illustration of the various coordination polyhedra observed in the anion of type **v**: central $[(\mu_6\text{-Se})Mn_6]$ octahedron (b), non-bonded $[(\mu\text{-Se})_{12}]$ cubo-octahedron (c), super-octahedron of six face-sharing $[Mn(\mu\text{-Se})_5(OH_2)]$ octahedra (d), face-sharing of four $[GeSe_4]$ tetrahedra with the $[(\mu_6\text{-Se})Mn_6(\mu\text{-Se})_{12}(OH_2)_6]$ super-octahedron (e).

the examples that have been obtained by further synthetic approaches (**I–III**), it becomes obvious that the counterion plays the most significant structure-directing role. This meets the expectations, since the high dependency of the structure of a complex anion on the nature of the cation A^{n+} – *i.e.* its radius:charge ratio r/n – is well known, e.g. for the synthesis of zeolitic materials [69]. However, there seems to be some tolerance for each structure type, such as for a given charge of A, one observes one complex type down to a lower limit of the radius:charge of the cation A^{n+}. Therefore, complexes of the type $[M_4E'_4E_{17}]$ (**4–8**, **I–II**) are observed with K^+, Rb^+ or Cs^+ (r/n: 138, 152, or 167 pm), whereas with Na^+ (r/n: 102 pm) or Ba^{2+} (r/n: 67.5 pm) this type of ternary anion does not seem to be sufficiently stabilized by the counterion network and another one is preferred (**9**, **10**). However, it is also necessary to take into consideration the size and thus the "bite" of the $[E'E_4]^{4-}$ groups – since these represent the counterpart for the cationic charge – and to correlate this with the steric demand of $[ME_4]$ tetrahedra or $[ME_6]$ octahedra. Therefore, ternary anions that contain "smaller" $[GeE_4]^{4-}$ groups may show different structures (except the dinuclear type **i**), due to the smaller bite of the 14/16 tetrahedra[3] and, *vice versa*, Na^+ ions may stabilize a P1-type cluster anion which contains $[SiO_4]^{4-}$ groups. In different structures, different charge densities result on the cluster surface. In $[SiO_4]^{4-}$ or $[GeE_4]^{4-}$ complexes, which possess relatively small volumes, this is best compensated for with a cation of a higher charge density. Among the cations explored so far, in the chemistry of M/14/16 anions, Ba^{2+} has the highest charge density and is therefore well suitable for the stabilization of M/Ge/Se anions. However, it may also serve to replace

---

[3] Experimentally observed E–E distances within ternary anions ("bite" of the $[E'E_4]^{4-}$ groups, i.e. measure for the volume of the $[E'E_4]^{4-}$ tetrahedra) are for different E′/E combinations—Si/O: 2.6–2.8 Å; Ge/S: 3.3–3.8 Å; Ge/Se: 3.7–3.9 Å; Sn/S: 3.8–4.0 Å; Sn/Se: 4.0–4.3 Å; Sn/Te: 4.3–4.6 Å.

a double amount of Na^+ ions from a certain M/Sn/S anion to obtain the appositely larger M/Sn/Se analogue (**10** versus **9c**). In addition to the pure steric consideration, it seems necessary to regard the extent of hydration, *i.e.* the amount of solvent molecules that are coordinated to both cations and anions. P1 type anions prefer a smaller hydration shell; therefore, they are well stabilized by the "softer" cations K^+, Rb^+ or Cs^+, which are also solvated to a lesser extent; this is naturally carried to an extreme for the H_2O-free phases $A_{10}[M_4Sn_4S_{10}]$ that were isolated from polychalcogenide fluxes [48,49]. Unlike this, the T3 type anion, bearing a larger hydration shell, prefers crystallization with the "harder", but more effectively solvated cations Na^+ or Ba^{2+}.

Another structure-directing parameter is the nature of the transition metal compound used for the synthesis. Naturally, the anionic structure of the finally crystallizing product is determined by the charge of the transition metal cation, which counts for the total charge and thus the crucial surface charge of the M/14/16 unit. The charge itself may change due to redox processes that can occur during the reaction if the respective redox potentials allow for this. As an example, Co^{2+} ions are released from a $[Co(en)_3]^{3+}$ complex upon reduction by S^{2-} or Se^{2-} ions in basic solution ($E^0_{1/2}$ in basic solution [V]: −0.18 V for $[Co(en)_3]^{2+/3+}$ [70a]; −0.476 for $S^{0/2-}$ [70b]; −0.92 for $Se^{0/2-}$ [70b]). In contrast, a $[Cr(en)_3]^{3+}$ behaves differently, since the Cr^{3+} centers are neither reduced ($E^0_{1/2}$ in basic solution [V]: −0.21 for $[Cr(en)_3]^{2+/3+}$) [70], nor do they liberate all *en* ligands like the cobalt analogue as a consequence of higher complex stabilities.

Therefore, different structures of the ternary anions are the consequence, allowing for the observation of the smallest, *en* containing complexes **1**–**3**. The size of the transition metal cation (usually doubly charged) and the chalcogen ligand only show minor structure-directing influence. The first may be viewed as an exclusion factor: the size of M^{n+} decides whether an anion may in principle be formed together with a certain type of $[E'E_4]^{4-}$ or not, but the product to be isolated in crystalline form – which might coexist with further possible anions in solution – is definitely selected by the counterion. The second is mainly responsible for the quality of the crystals: certain combinations of A and E lead to stronger coordination interaction than other. For instance, the combination Na/S is favored for crystallization over Na/Se, Cs/Te is advantaged with respect to Cs/S, according to the principle of hard and soft acids and bases (HSAB) [71]. It is not clear yet why some of the compounds reproducibly incorporate further ions, while others seem to be adequately stabilized by the number of counterions that are needed to compensate for the anion's charge besides solvent molecules. It is, however, evident that an optimization of the lattice energy gain is the general driving force for the crystallization using extra-ions such as Cl^-, $[Cr(en)_3]^{3+}$, the reactant $[SnSe_4]^{4-}$, its dimerization product $[Sn_2Se_6]^{4-}$, Eq. (1), or the product of a partial hydrolysis that the lighter homologue germanate anions undergo in aqueous solution, $[GeS_3OH]^{3-}$, Eq. (2):

$$2\,[SnSe_4]^{4-} \overset{aq}{\rightleftarrows} [Sn_2Se_6]^{4-} + 2\,Se^{2-} \tag{1}$$

$$[GeS_4]^{4-} + H_2O \overset{aq}{\rightleftarrows} [GeS_3(OH)]^{3-} + HS^- \tag{2}$$

Moreover, a comparably high complexity of the crystalline products exclusively was observed upon synthesis in solution (Scheme 6), which suggests that this preparation technique might allow, in principle, for even a higher variety of observable compounds than the alternative routes at high(er) temperatures.

The most complex counterion aggregates that were observed with these compounds containing molecular M/14/16 anions are those of compounds **1** and **5**. Figs. 6 and 7 show views of the resulting unit cells.

In **1**, there are two types of singly charged ions (Na^+ and $[Cr(en)_2(GeSe_4)]^-$) and two triply charged species ($[Cr(en)_3]^{3+}$ and $[GeS_3(OH)]^{3-}$). These are arranged in layers of singly charged or triply charged ions, respectively, parallel to the *bc* plane. The two types of layer themselves interact, as usual, *via* the solvent H_2O molecules, being linked by them by hydrogen bridges or Na···O coordination.

The crystal structure of compound **5** also hosts four types of different ions: K^+, Cl^-, $[SnSe_4]^{4-}$ and the ternary $[Co_4(\mu_4\text{-}Se)(SnSe_4)]^{10-}$. As usual, K^+ ions are coordinated by solvent (H_2O and MeOH) molecules and Se ligands of the anions (binary and ternary here). This way, they act as "glue" between the anions, stabilizing the salt. However, this compound not only uses binary anions $[SnSe_4]^{4-}$ for an appropriate crystal lattice, as observed in several cases, but also incorporates Cl^- in a most noticeable way as can be seen in Fig. 7b and c: the bulk of ternary anions, K^+ cations and solvent molecules is interrupted by layers that contain parallel zigzag chains of alternating $[K_9Cl_2]^{7+}$ and $[SnSe_4]^{4-}$ units. The first represent two face-sharing $[K_6(\mu_6\text{-}Cl)]$ octahedra, *i.e.* the smallest fragments of the KCl structure are linked in a way that they would not lead to three-dimensional crystal packing.

Some of the compounds mentioned above with molecular anions (see Section 3.1) have a very high formation tendency, being represented by both high yields and a high tolerance for varying reaction conditions. In these cases, e.g. the syntheses of **6a** or **8a**, the stoichiometry of the reactants and the composition of the solvent mixture (H_2O and MeOH in different ratios) only affect crystal quality and yields; in contrast, there are some systems which respond to a variation of these parameters by crystallization of different compounds. As far as the nature of the solvent is concerned, this can be taken as a hint for the coexistence of different species in solution, the less soluble of which, under the given condition, will precipitate. In addition, this shows the importance of further, competing processes to be considered. The most evident side reaction is the formation of binary transition metal chalcogenides M_nE_m. This naturally plays an increasing role with decreasing solubility of M_nE_m and is both dependent on the nature of the solvent and the concentration of the reactants. The respective systems additionally seem to show smaller differences in the stability or solubility of different compounds with ternary anions. As an example, reactions of $[SnSe_4]^{4-}$ with Hg^{2+} salts, which produce a significant amount of HgSe and accordingly provide lower yields of quaternary phases, allow for the isolation of three different

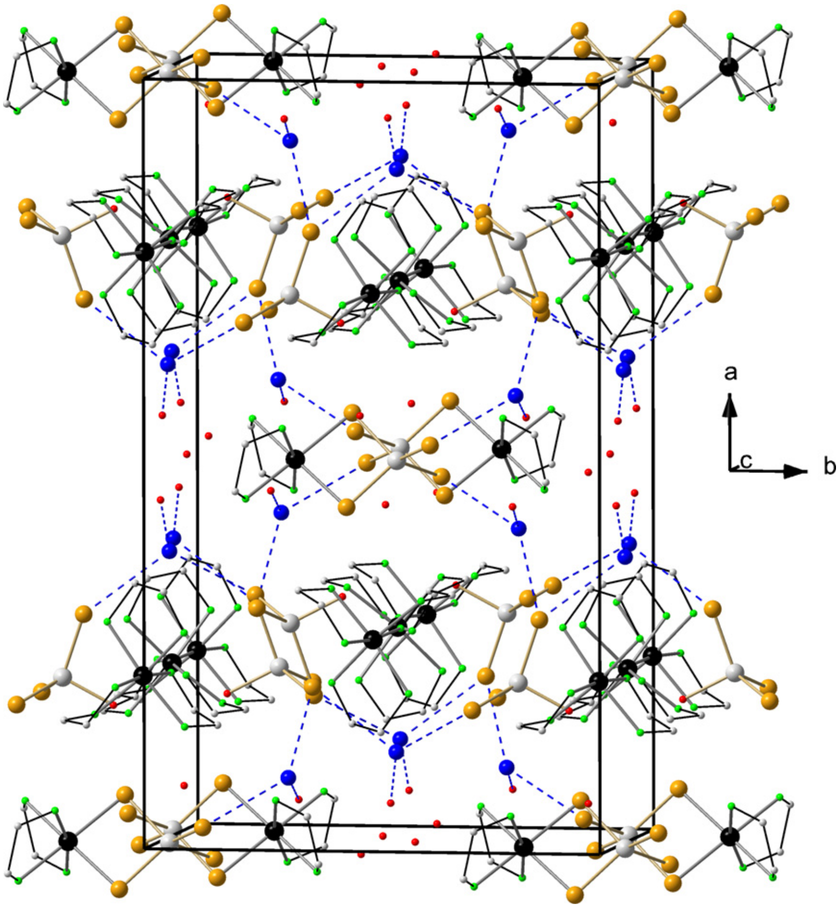

Fig. 6. Unit cell of **1** [29], showing the layered arrangement of singly and triply charged anions. Na···S and Na···O contacts are given by dashed lines [S: yellow; Sn: light grey; Na: blue; C: light grey; O: red; N: green; Cr: black].

products, **6d**, **14**, and **18**. In the last two cases, as well as in further reactions yielding compounds **15–17**, it was indeed possible to obtain coordination polymers containing the $[E'E_4]^{4-}$ units *via* reactions of *ortho*-chalcogenotetrelate anions in solution. Probably less surprisingly, the two phases that have formed in reactions of *ortho*-chalcogenotetrelate anions with transition metal compounds under *solvothermal* conditions (**19a** and **19b**) also contain polymeric M/14/16 anions; similarly, some of the further polymeric structure types that are discussed below are also accessible via reactions of separate sources for M, E′, and E at higher temperatures via solvothermal or flux techniques (see below).

3.2. Crystal structures of compounds with polymeric M/14/16 anions

3.2.1. One-dimensional polymers

The ternary anions in compounds **14–16** and **19** represent one-dimensional strands of edge-sharing, alternating $[SnE_4]^{4-}$ and $[ME_4]^{6-}$ tetrahedra (type **vi**). These run through the crystal along one of the crystallographic axes and coordinate to interstitial alkali metal or ammonium cations via Te atoms. As for molecular anions of type **iii**, one has observed this polymer for a variety of A/M/Sn/E combinations so far, namely K/Hg/Sn/Se (**14**), K/Hg/Sn/Te (**19a**), Rb/Hg/Sn/Te (**15**), and Cs/Mn/Sn/Te (**16**). Fig. 8 shows a fragment of the crystal structure in **15**, as an example, and depicts a fragment of a one-dimensional anionic strand.

Different coordination environments of the alkali metal cations (that cause different relative orientations of the parallel strands that may be shifted against each other in the direction of the polymer) allow for the stabilization and thus crystallization of variations of M/Sn/E strands in spite of different relative sizes of the involved atom types: isostructural arrangements were observed for Hg compounds **14** and **15**, crystallizing tetragonally with K/Se or Rb/Te as coordination partners. Increasing the radius of the cation (Cs) or decreasing the transition metal atomic size (Mn) provokes a structural answer which is found in the different, orthorhombic crystal structure of **16**. The preference for the formation of type **vi** anions under the given conditions, *i.e.* the given elemental combination and solvent, is further underlined by an ion exchange experiment in *en*, yielding compound **19b** with unaffected $[HgSnTe_4]^{2-}$ strands in modified relative orientation upon substitution of $[NEt_4]^+$ for K^+. Uniquely, and independent from the preparation technique, solvent molecules seem either to be not necessary or not tolerable in these types of quaternary phases.

Further one-dimensional strands have not been observed using the coordination chemical approach, but by reacting separate components in an alkali-metal polychalcogenide flux,

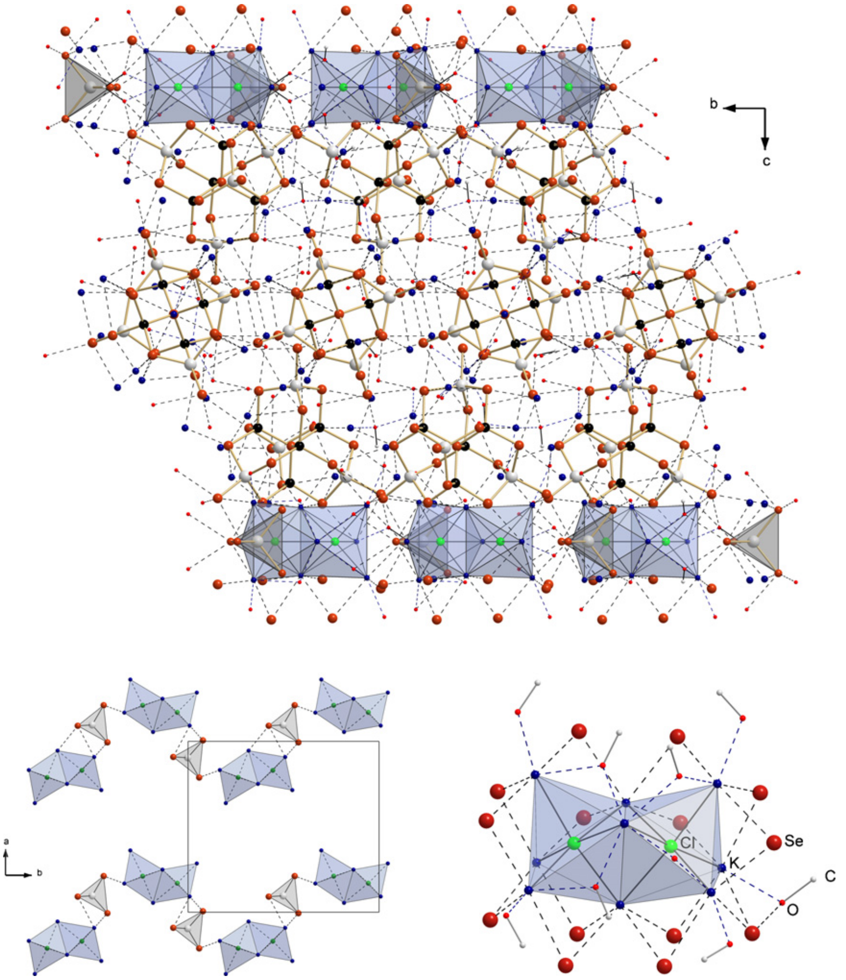

Fig. 7. Crystal packing diagram of compound **5** (top) [31], polyhedral representation of zigzag chains of alternating $[K_9Cl_2]^{7+}$ and $[SnSe_4]^{4-}$ units in the cell of **5** (bottom, left) and zoom of one $[K_9Cl_2]^{7+}$ unit within its coordination sphere (bottom, right) [Se: red; Sn: light grey; K: blue; C: light grey; O: red; Cl: green; Co: black].

anions containing $[E'E_4]^{4-}$ or $[Sn_2E_6]^{4-}$ linked transition metal atoms have been generated. A structure which is very similar to type **vi** is present in compound $K_2[MnSn_2Se_6]$ with Mn^{2+}-linked $[Sn_2Se_6]^{4-}$ units [72]. Three further examples of related compounds that contain gold complexes have been prepared by polychalcogenide flux synthesis or high temperature reactions, respectively: $BaAu_2SnS_4$ (**IV**) [73a], $K_2Au_2SnS_4$ (**V**) [73b] and $K_2Au_2Sn_2S_6$ (**VI**) [73b]. In these, units of two gold atoms with relatively short Au–Au distances (297–336 pm) are linearly coordinated by S-atoms of $[Sn_xS_y]^{4-}$ units ($[SnS_4]^{4-}$ in **IV** and **V**, $[Sn_2S_6]^{4-}$ in **VI**), thereby generating one-dimensional chains. In $K_2Au_2Sn_2S_6$ and $BaAu_2SnS_4$, Sn atoms are positioned in a straight line (**IV** according to type **vi** with $[Au_2]^{2+}$ dumbbells instead of single M^{2+} ions), while they are arranged in a zigzag fashion in $K_2Au_2SnS_4$ ($\angle Sn\cdots Sn\cdots Sn$: 107.46(6)°) (Fig. 9).

Straight versus zigzag strand formation can again be put down to counterion effects: only $[Sn_2S_6]^{4-}$ units provide enough space to accommodate the required number of K^+ cations for charge compensation. When replacing the dimeric units by monomeric $[SnS_4]^{4-}$ tetrahedra, doubly charged Ba^{2+} cations fit equally, whereas in the corresponding K^+ salt a zigzag pattern of the chain is needed for good crystallization. Another, more complicated M/14/16 strand was prepared by *en*-extraction of a multinary alloy by Haushalter et al., who published the structure and properties of the semiconducting, mixed-metal tellurostannate compound $[NEt_4]_4[Au(Ag_{1-x}Au_x)_2Sn_2Te_9]$ (E_{gap}: 0.45 eV) [74a]. Here, corrugated strands are formed by linkage of $(Au/Ag)_2Te$ units and Au atoms by $[SnTe_4]^{4-}$ groups, including a nearly linear $\{Au–Te–Te–Te\}_n$ chain. The preference for coin metal atom aggregation is further reflected in the recently published silver thiostannate $[1,4\text{-}dabH_2][Ag_2SnS_4]$ (1,4-dab = 1,4-diaminobutane), containing unusual one-dimensional strands of $[SnS_4]$-linked groups of four Ag atoms [74b]. It is also possible to obtain one-dimensional strands using $[E'_xE_y]^{q-}$ anions with a higher degree of condensation. A double chain with linked $[Ge_4S_{10}]^{4-}$ units was prepared by the *Parise* group via solvothermal reaction of GeS_2, Dabco and $Ag(OAc)_2\cdot 4H_2O$ (Fig. 10) [74c].

In $[(C_6H_{13}N_2)_2(H_3O)(H_2O)][AgGe_4S_{10}]$ (**VII**), double chains of $[Ge_4S_{10}]^{4-}$ units are formed by trigonal planar coordination of Ag^+ ions to all three of these units. Instead of further linkage into two- or three-dimensional networks, one terminal S ligand of the $[Ge_4S_{10}]^{4-}$ groups remains at a terminal position.

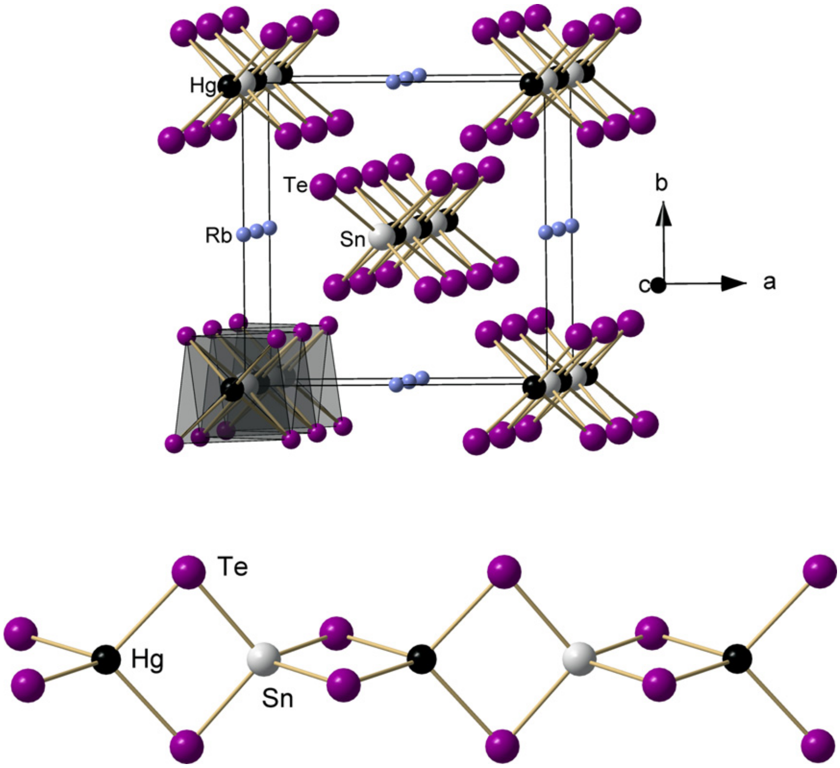

Fig. 8. Crystal packing diagram of compound **15** (top) [35] and fragment of a one-dimensional anionic strand (bottom) as an example for type **vi**.

3.2.2. Two-dimensional polymers

Using very similar conditions, at least using the same counterion, one understands a structural relationship of some of the polymers to the respective molecular anions: the extended M/14/16 anionic substructures of compounds **17** and **18** can clearly be derived from those of compounds **11** and **6d**, respectively. A yet unprecedented two-dimensional anionic network is observed in compound **17** upon substitution of three terminal selenium atoms of three adjacent cluster units for three of the six coordinated water molecules (at the discrete cluster unit in **11**). *Vice versa*, three of the terminal Ge-bound selenium atoms of the central cluster unit coordinate to former O-coordination sites of the same neighboring clusters. By continuation of this process, one obtains corrugated, honeycomb-type layers

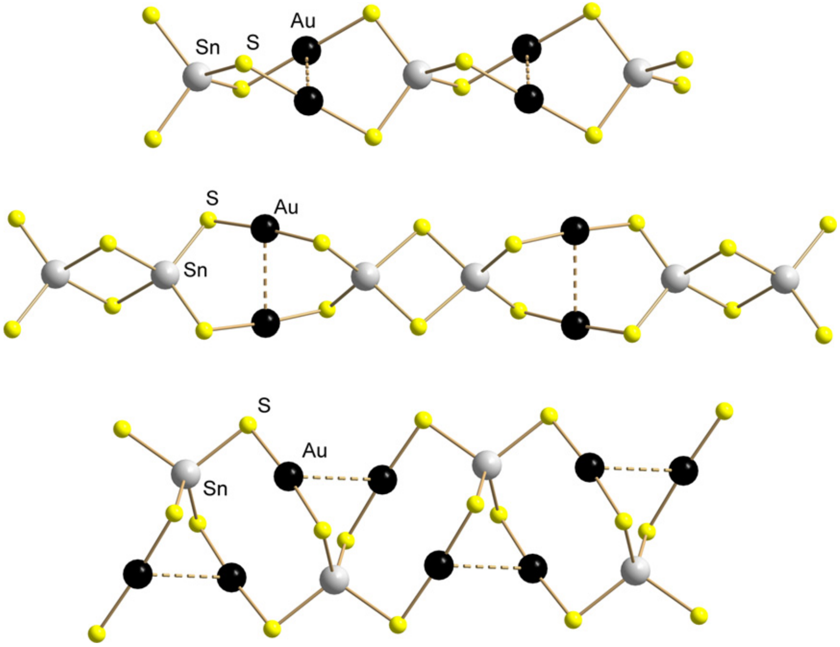

Fig. 9. View of one-dimensional anionic strands in compounds $BaAu_2SnS_4$ (**IV**, top) [73a], $K_2Au_2Sn_2S_6$ (**V**, middle), and $K_2Au_2SnS_4$ (**VI**, bottom) [73b].

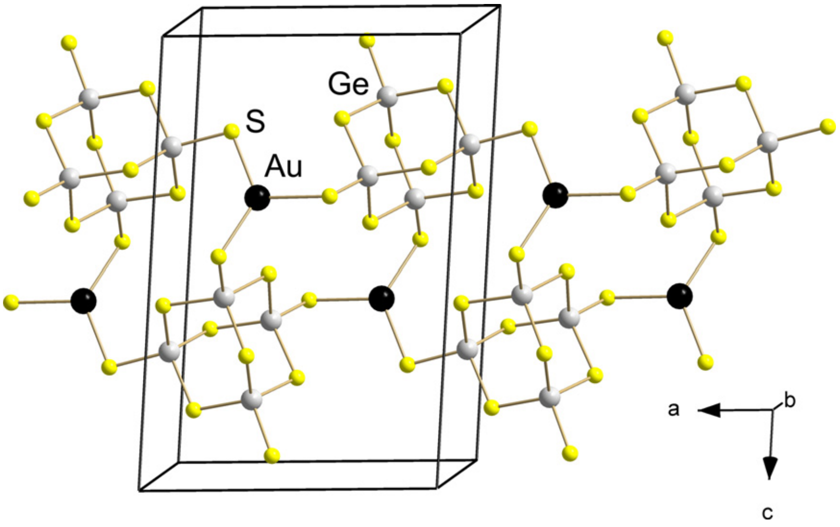

Fig. 10. Double chain of $[Ge_4S_{10}]^{4-}$ anions and trigonally coordinated Ag^+ ions in **VII** [74c].

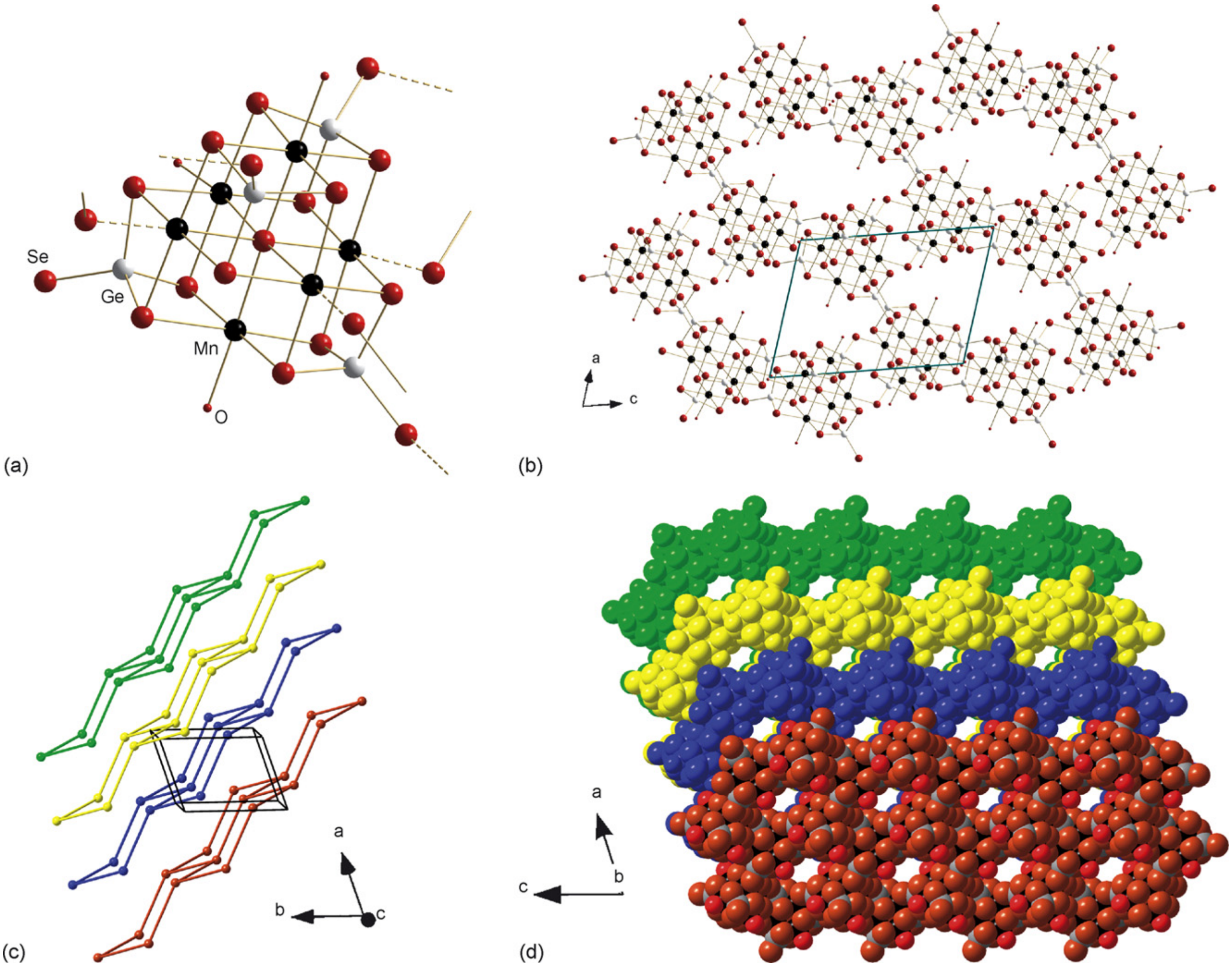

Fig. 11. Structure of the ternary anion in **17** (type **vii**; broken bonds represent bonds to adjacent cluster units) (a) and its formal condensation into a layered coordination polymer (b) [26]; different representations of the packing of the two-dimensional layers: linkage of cluster centers within four layers viewing down the *c* axis to illustrate the topological relationship to the structure of gray arsenic (c); space-filling representation of four stacked layers viewing down the *b* axis (d).

of linked cluster units (type **vii**). These layers are stacked parallel to [0 1 0], the packing resembling that in grey arsenic at larger scale. Although the honeycomb pores show diameters of approx. 7.5 and 14.5 Å, the staggered arrangement of the layers nearly leads to complete coverage of the pores. The remaining channels parallel to the crystallographic axis b show maximum diameters of approx. 3.5 Å. Naturally, counterions (Ba^{2+}) and solvent molecules (H_2O) are situated within those channels and between the anionic layers, acting as both template-like, directing and stabilizing species in the generation of the M/14/16 substructure (Fig. 11).

So far, compound **17** is the only one observed by the coordination chemistry route to form a layered anionic substructure. Being rare for this type of approach, the formation of layers is quite common for different synthetic routes, such as for polysulfide flux syntheses or solid state reactions from binary sulfides. Numerous salts were isolated and structurally characterized – particularly in the 1970s and the 1980s – the ternary anionic substructures of which represent corner sharing and/or edge sharing tetrahedra $[E'S_4]$ and $[MS_4]$. Examples of products that were formed from these flux or fusing reactions are $Rb_2[Cu_2SnS_4]$ [73b], or $Ba[CdSnS_4]$ [73c], respectively. Another related compound that has recently been prepared by solvothermal synthesis is $[Zn(C_6N_4H_{18})(H_2O)][Zn_2(H_2O)_2Ge_3S_9]$ [75] (Fig. 12).

Here, T2-type $[Zn(H_2O)Ge_3S_6(S_{1/2})_3]$ clusters are cross-linked by $[Zn(H_2O)S(S_{1/2})_2]$ tetrahedra, three of which act as bridges to three adjacent T2 clusters *via* common sulfur atoms, resulting in planar sheets with triangular holes. This porous wide-band semiconductor compound (E_{gap}: 3.6 eV) shows photocatalytic activity for the production of H_2 from aqueous Na_2SO_3 solutions.

3.2.3. Three-dimensional polymers

The anionic substructure in compound **18** (type **viii**) can formally be obtained upon removing one $[SnE_4]^{4-}$ unit from a P1-type cluster anion and subsequent re-saturation of the free coordination site of each of the three Hg atoms by a terminal chalcogen atom E of an adjacent, identical cluster fragment. Three-dimensional continuation of this formal condensation process generates a polymeric network with the packing of the linked cluster fragments resembling the cubic primitive α-Po type at larger scale. Accordingly, three orthogonal series of parallel channels with maximum diameters of approx. 4×7 Å^2 (**18a**, E = Se) or approx. 4.5×8 Å^2 (**18b**, E = Te) are observed that enclose counterions and solvent molecules (Fig. 13).

Whereas compounds containing discrete anions of type **iii** show a broad tolerance regarding the M/14/16 composition, the polymeric derivative has only been observed with group 10 transition metals. Compounds **18a** and **18b** are the only examples which were obtained by a coordination chemistry route; two further, solvent free examples of type **viii**, $K_6[Cd_4Sn_3Se_{13}]$ (**VIII**) [76a] and $K_3Rb_3[Zn_4Sn_3Se_{13}]$ (**IX**) [76b], were prepared under solvothermal conditions using K_2Se and separate sources for group 10 metal, selenium and tin. A recent attempt to convert compound **VIII** into its solid acid "$H_6[Cd_4Sn_3Se_{13}]$" – in analogy to the formation of solid-acid, catalytically active zeolites [77] – surprisingly led to a reassembly to give the phase $K_{14}[Cd_{15}Sn_{12}Se_{46}]$; the three-dimensional network, basing on the yet unprecedented, Se-linked units $[Cd_5(Sn_2Se_7)_2(\mu_3\text{-}Se)_{4/3}]^{14/3-}$, is able to take up different cations upon cation exchange reaction [78a]. Another three-dimensional variation of type **iii** cluster anions is present in the anionic substructure of compound $K_6\{Sn[Zn_4Sn_4S_{17}]\}$ prepared by Kanatzidis et al. Here, intact P1-type clusters are linked via their terminal S-atoms by four-fold coordinated Sn^{4+} ions, thus forming a three-dimensional network [78b].

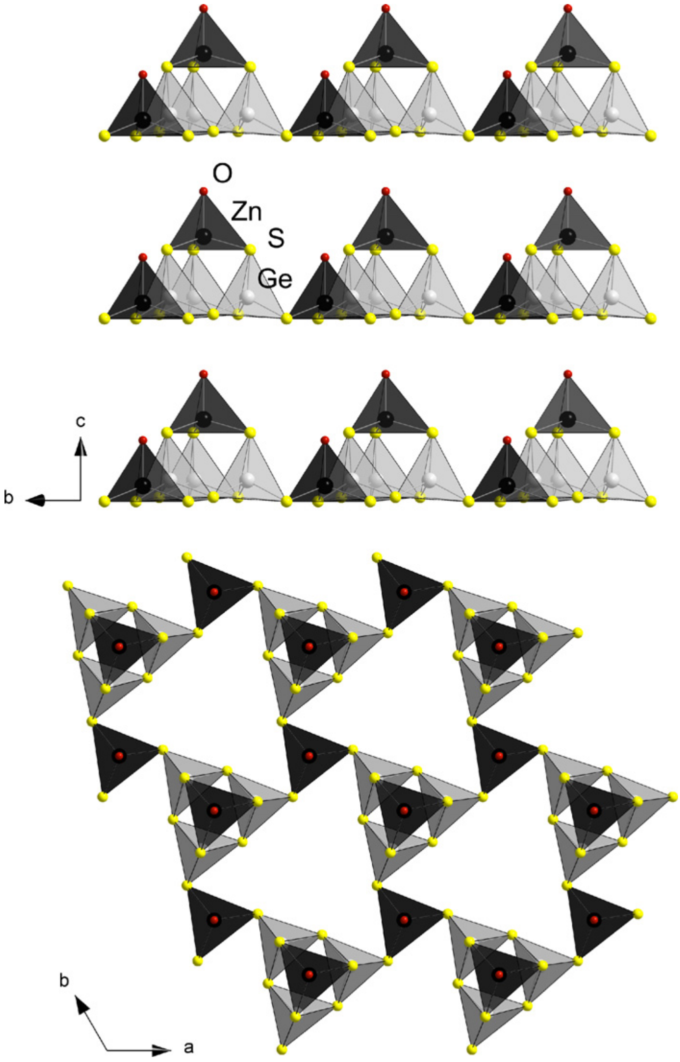

Fig. 12. Side view (top) and top view (bottom) of anionic $\{[Zn_2(H_2O)_2Ge_3S_9]^{2-}\}_n$ layers observed in $[Zn(C_6N_4H_{18})(H_2O)][Zn_2(H_2O)_2Ge_3S_9]$ [75].

A very common type of anionic polymers, being observed at first with the solution method's pioneer compound **12a**, is the "open framework" structure of the general type $[MGe_4E_{10}]^{2-}$ (type **ix**, compounds **12** and **13**). In contrast to the anionic double strands in compound **VII** mentioned above [75], adamantine-type anions $[Ge_4E_{10}]^{4-}$ share μ-E atoms with tetrahedral $[ME_4]^{q-}$ units to form a defect-sphalerite type architecture (Fig. 14a) with a diamond-type arrangement of the barycenters of linked $[Ge_4E_{10}]^{4-}$ and $[ME_4]^{q-}$ units, respectively (Fig. 14b).

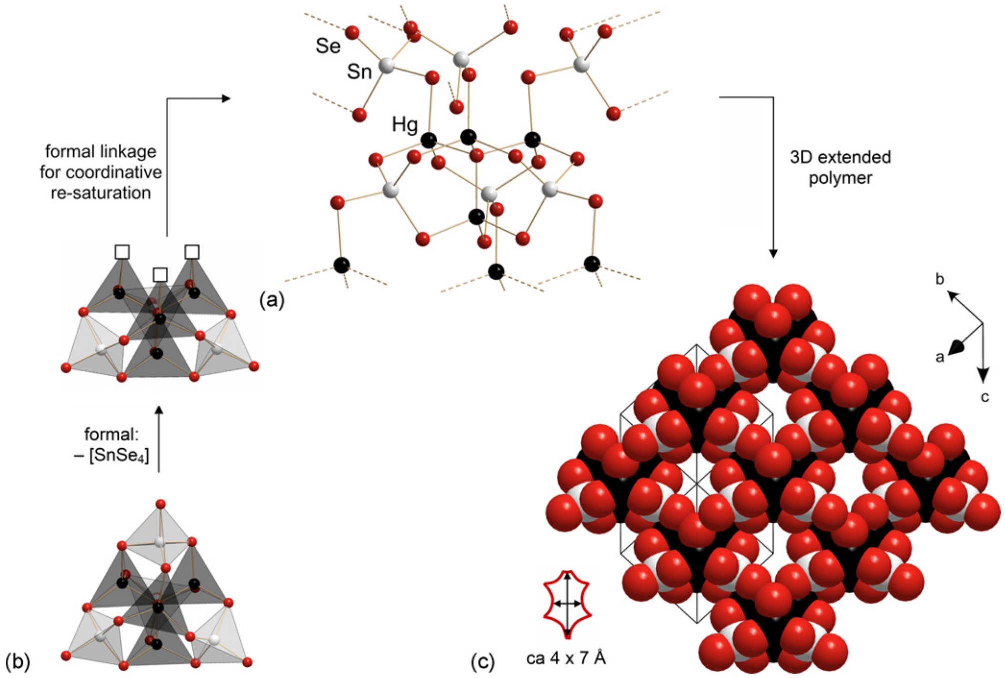

Fig. 13. Structure of the ternary anion in **18a** (type **viii**; broken bonds represent bonds to adjacent cluster units and continuation of the structural motif) (a) [32]; derivation of a monomeric "$[Hg_4(\mu_4\text{-}Se)(SnSe_4)_3]^{6-}$" unit in **18a** by formal removal of an $[SnSe_4]^{4-}$ group from a discrete $[Hg_4(\mu_4\text{-}Se)(SnSe_4)_4]^{10-}$ anion in **6d** (b); formal polymerization to form the anionic Hg/Sn/Se network in **18a** (c), space-filling representation viewed approximately along [1,−1,−1].

This framework has been observed with numerous combinations of M (Mn, Fe, Cu_2, Ag_2) and E (S, Se), and even with a remarkably variety of counterions A (K, Rb, Cs, NMe_4) [18,21,22,79]. The different variations of compounds **12** and **13** – except **13c** – were synthesized using salts of the $[Ge_4E_{10}]^{4-}$ anions, whereas further examples, namely $A_3[AgGe_4Se_{10}]\cdot 2H_2O$ (A = Rb, Cs; **Xa**, **Xb**), $A_2[MnGe_4Se_{10}]\cdot 3H_2O$ (A = Rb, Cs; **Xc**, **Xd**) [79], were obtained by hydrothermal reactions of separate sources for A, M, Ge and E. Most of the compounds quoted have been obtained as powders or microcrystals; however, using isotypic **12a** as a model, it was possible to structurally characterize these in spite of their relatively complicated crystal structure. Recently, we added the yet missing potassium salt as its solvate **13c**. Thus, the accepted value of the effective counterion radius ranges from 251 pm for $[NMe_4]^+$ [80] in **12**, **13a** or **13b**, down to 160 pm for seven-coordinate K^+ [81] in **13c**.[4]

Both the large counterion tolerance and the very different synthetic routes that lead to these isotypic compounds indicate the high preference for this anionic network. The unexpected synthesis of **13c** may additionally confirm this statement: although reacting $K_4[GeSe_4]$ with $MnCl_2\cdot 4H_2O$ in H_2O, one observes the incorporation of the tetramerization product (Eq. (3)) of originally used *ortho*-chalcogenotetrelate anions within the product network:

$$4[E'E_4]^{4-} \overset{aq}{\rightleftarrows} 2[E'_2E_6]^{4-} + 4E^{2-} \overset{aq}{\rightleftarrows} [E'_4E_{10}]^{4-} + 6E^{2-} \qquad (3)$$

The only further pattern of $[E'_4E_{10}]^{4-}$ and $[ME_4]^{q-}$ linkage to be determined by single crystal X-ray analysis was observed upon hydrothermal synthesis of $[C_6H_{14}N_2][MnGe_4S_{10}]\cdot 3H_2O$ (**XI**) [82] in the presence of bicyclic *Dabco* amine, which was transferred in situ into the bulky H_2*Dabco* counterion. Here, the network topology resembled that of the zeolite Li-A(BW) [83], when formally substituting $[Ge_4S_{10}]^{4-}$ or $[MnS_4]^{6-}$ groups for the $[SiO_4]^{4-}$ or $[AlO_4]^{5-}$ units, respectively, in the zeolite. Both topologies are opposed to each other in Fig. 15.

However, the presence of again bulkier cations, such as $(MesMe_3N)^+$ or long chain surfactant molecules, forces the structures to form larger cavities. The powders obtained (compounds **20**–**27**) have not yet been structurally characterized, but all the analytical information available to date suggest metal bridged anions $[E'_xE_y]^{4-}$ to form a variety of mesoporous networks with pore sizes between 30 and 40 Å [23,24,38–44]. These show promising opto-electronic properties in addition to large material surfaces, which led to investigations that point towards photochemical or photocatalytic applications.

3.3. *Physical properties*

3.3.1. *Optical absorption behavior*

Due to their elemental composition, which represents a formal mixture of main group chalcogenide and transition metal chalcogenide derivatives, opto-electronic properties are an exciting matter of investigation when studying compounds that contain ternary M/14/16 anions. Therefore, most of the compounds presented herein were investigated by UV–vis spectroscopy. Owing to the significance of these salts with respect to material application, the optical absorption behavior of these

---

[4] Note that the presence of two or three water ligands per three or two cations in **Xa**, **Xb**, or **13c** does not significantly increase the effective radius; the counterions are mainly coordinated by E ligands in all cases.

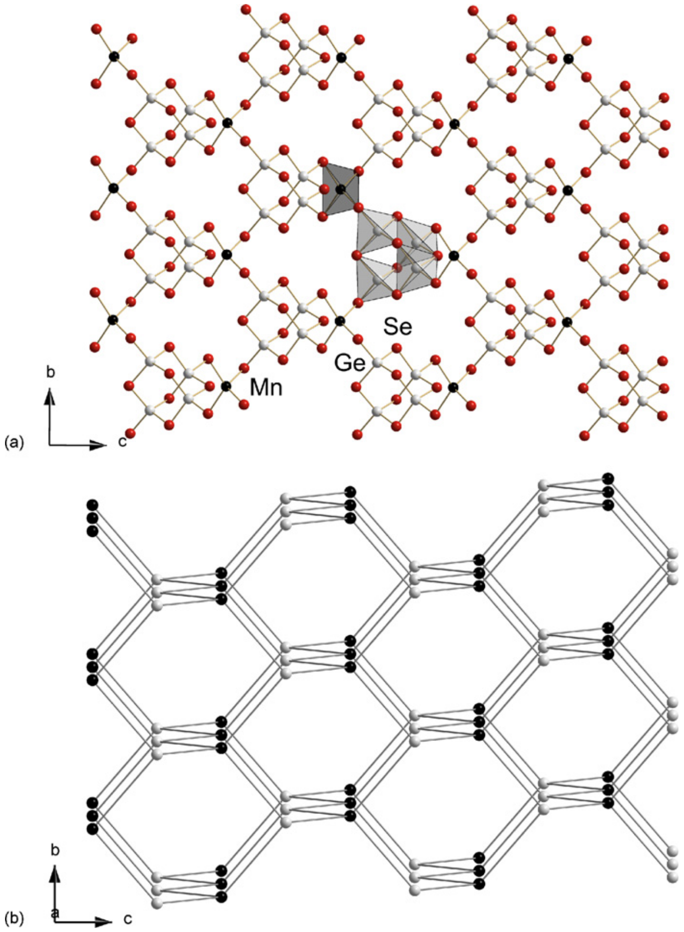

Fig. 14. “Open framework” structure of the type **ix** anionic Mn/Ge/Se network in **13c** [35] as an example for compounds **12** and **13**: (a) one T1 and one T2-tetrahedron are emphasized by polyhedral representation; (b) representation of the barycenters of the junct $[Ge_4E_{10}]^{4-}$ and $[ME_4]^{q-}$ units in compounds **12** and **13** highlighting the structural relationship to the diamond structure [18,21,22,35].

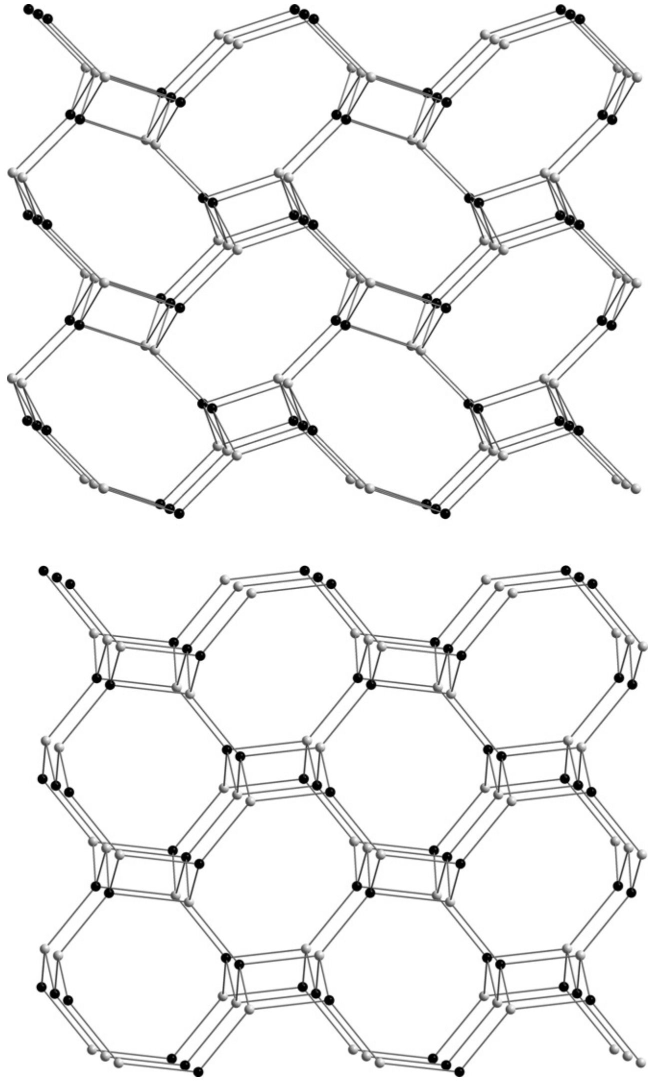

Fig. 15. Representation of the barycenters of the linked $[Ge_4S_{10}]^{4-}$ (grey spheres) and $[MnS_4]^{6-}$ units (black spheres) in compound **XI** (top) [82], highlighting its structural relationship to the respective linkage of $[SiO_4]^{4-}$ (grey spheres) and $[AlO_4]^{5-}$ units (black spheres) in zeolite Li-A(BW) (bottom) [83].

compounds was usually investigated in the solid state. For d^n ($n \neq 0$) complexes, d–d bands are usually superposed by charge transfer transitions of the highly absorbing $[E'_xE_y]^{q-}$ groups. However, for compounds **1**–**3**, containing mononuclear or dinuclear type **i** or **ii** Cr^{3+} complexes, the absorption characteristics clearly reflect the presence of various chromophores.

In accordance with their brown color, crystals of **1** show absorption over the whole visible spectral range, however, retracing the absorption of the components $[GeS_4]^{4-}$, $[Cr(en)_3]^{3+}$ and $[Cr(en)_2Cl_2]^{+}$. Chemically modified, an appropriate shift of the absorption is observed for **1** with respect to the pure components (Fig. 16a).

Similar observations are made for compound **3**: again, the dark appearance of the crystals is reflected by absorption over the whole visible range of the spectrum (Fig. 16b). As expected from the darker color of the crystals when compared to **1**, the onset of absorption and the maximum absorbance are reached at lower energies than with the Na/Cr/Ge/S compound. For **3**, only one shoulder is observed at 1.85 eV, in accordance with only one type of Cr^{3+} center present in this salt. Upon substitution of (weaker) $[GeSe_4]^{4-}$ ligands for (stronger) H_2O ligands, the shoulder is red-shifted with respect to the respective lower energy absorption band of $[Cr(en)(H_2O)_4]^{3+}$ (512 nm, *i.e.* 2.42 eV) [84].

Most of the polynuclear, $[E'_xE_y]^{q-}$ coordinated transition metal complexes – except the Co compounds – exhibit essentially featureless, step-like absorption spectra. These represent LMCT, MLCT or MMCT processes according to theoretical investigations. For a given anionic structure type within the salts, the observed onset of absorption, which corresponds to the lowest possible electronic excitation energy, E_g, depends mainly on both the nature of the transition metal M and the nature of the chalcogen E. This is illustrated, for example, by the series $[K_{10}(ROH)_n][M_4(\mu_4\text{-}E)(SnE_4)_4]$ (R = H, Me; M = Zn, Mn, Cd, Hg; E = Se, $n = 16.5$ (**6**) or Te, $n = 20$ (**8**)) in Fig. 17.

Relatively small electronic excitation energies for the given molecular size (25 cluster atoms) are observed, although only

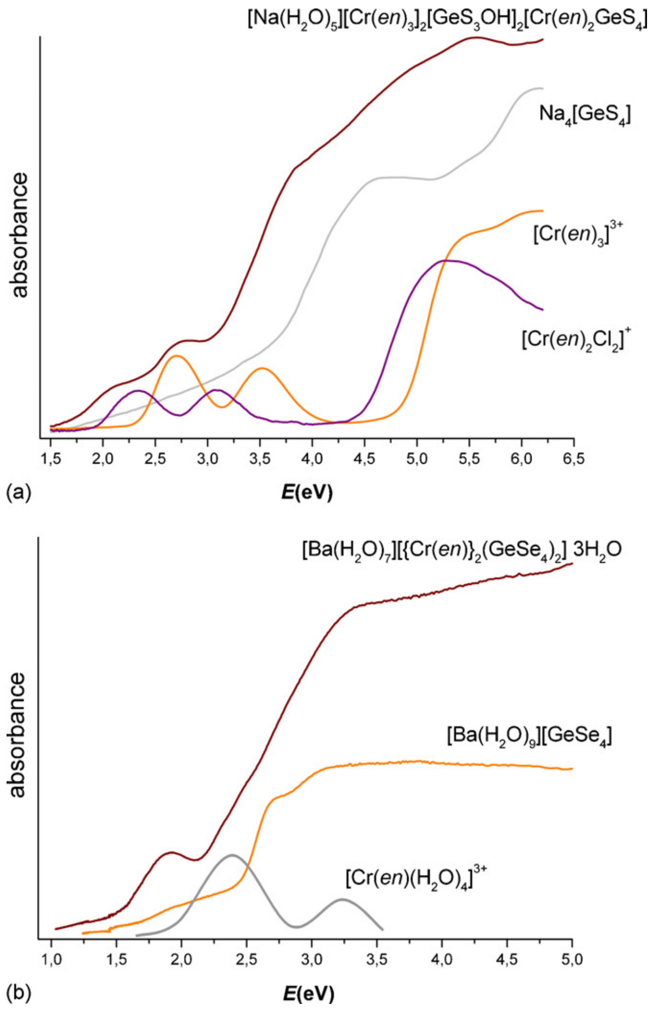

Fig. 16. UV–vis spectra of $[Na(H_2O)_5][Cr(en)_3]_2[GeS_3OH]_2[Cr(en)_2GeS_4]$ (**1**) (a) and $[Ba(H_2O)_7][\{Cr(en)\}_2(GeSe_4)_2]\cdot 3H_2O$ (**3**) (b) as well as UV–vis spectra of compounds representing components of the complex salts [29].

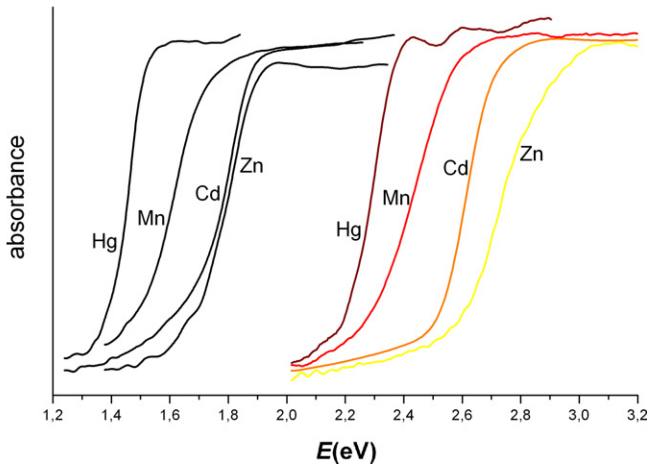

Fig. 17. Series of UV–vis spectra of compounds containing P1-type anions (type **iii**) $[K_{10}(ROH)_n][M_4(\mu_4\text{-}S)(SnE_4)_4]$ for M = Zn, Mn, Cd, Hg and E = Se (right hand side) [32] or Te (left hand side) [33].

very small (re-arranged) parts of the Wurzite type topology of the binary MSe phases [12] are represented by the inner $[(\mu_4\text{-}Se)M_4(\mu\text{-}Se)_{12}]$ cores of the ternary anions. The E_g values are significantly smaller than for related $[M_8E_{17}]$ clusters, which can be put down to (a) partial substitution of Sn (optical gap of $SnSe_2$: 1.2 eV [12]) for the transition metal d^{10} atoms, which causes a significant change of the electronic situation, and (b) the absence of any organic ligand shell. Optical gaps that were observed for the related mesostructured compounds $(CP)_{4-2x}[M_xSnSe_4]$ (**25**) (M = Mn, Zn, Cd, Hg) are in a similar range (2.0–2.5 eV) [85]. This indicates that both separation of discrete M/Sn/Se anions by (solvated) K^+ ions and incorporation of large surfactant micelles in a three-dimensional aggregation affect the optical behavior in a similar manner. Besides the fine-tuning of the E_g values with the variation of M, one observes a red-shift when going from E = S through Se to Te. For the solvent-free quaternary sulfides **I** and **II**, the absorption energies are in the range of 1.8–3.16 eV. Although exhibiting the same M/Sn/S elemental combination, compounds **9a** and **9b** exhibit either smaller or similar absorption energies (1.3 eV for M = Co, 3.3 eV for M = Zn) when compared to compounds **Ib** and **Id**, respectively (1.8 eV for M = Co and 3.2 eV for M = Zn), which shows that the influence of different formulae or anionic topologies at the same M/E′/E elemental composition may be competed by further effects, such as the anionic packing. This is confirmed by investigation of the influence of different arrangements of the complexes within the crystal on the opto-electronic properties. Significantly closer proximity of the anions by formal linkage into extended two- or three-dimensional networks approaches the situation in a respective quaternary solid. This comes along with a decrease of E_g, as observed when comparing the excitation energies of **11** and **17**, for example: upon approach of the cluster units from discrete positions to layers (average distances between central μ_6-bridging Se atoms of adjacent anions are 13.4 Å in **11**, 12.7 Å in **17**) and by changing the coordination environment from $MnSe_5O$ to the weaker field of $MnSe_{5.5}O_{0.5}$ on average, E_g is red-shifted from 2.2 eV (**11**) to 2.0 eV (**17**) (Fig. 18).

Inspite consisting of molecular components, both absorption energies are similar to the optical gaps in the binary solids MnSe [12] and $GeSe_2$ [86] (2.5 eV both), again illustrating the band narrowing upon combining transition metal, tetrel and chalcogen.

3.3.2. *Magnetism*

Investigation of the magnetic behavior of A/M/14/16 compounds that contain paramagnetic transition metal centers revealed antiferromagnetic coupling of the spins via chalcogenide bridges.

Coupling of four Mn^{2+} ions in compound **6a**, five Co^{2+} ions in **9a**, six Mn^{2+} ions in **11** or a formally infinite number of Mn^{2+} ions in **16** showed that (a) antiferromagnetic coupling with complete compensation of spins ($S = 0$) at $T \to 0$ K is observed for an even number of M; (b) for an odd number of cations, as in **9a**, a remaining spin of $S = \frac{1}{2}$ at $T \to 0$ K reflects a strong tetrahedral field, which is unprecedented for Co–S complexes;

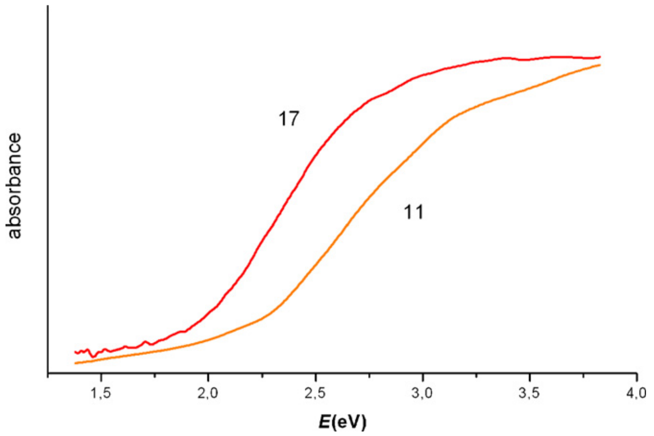

Fig. 18. UV–vis spectra of **11** (discrete anions, type **v**), and **17** (corresponding two-dimensional anionic network, type **vii**) [26].

(c) the desired antiparallel spin orientation is even realized via E–Sn–E bridges as in **16**.

Scheme 9 summarizes the so far investigated M/E arrangements within the ternary anions and possible (idealized) coupling pathways. Relevant χ^{-1}/T, χ/T or $\chi T/T$ diagrams are presented in Fig. 19.

The complicated topology of the magnetic pathways precludes a simple calculation of the cluster's spin levels by Kambe's method [87], hence a more general procedure developed by Clemente-Juan and co-workers (MAGPACK program) was used [88]. Whereas the magnetic coupling could be modeled in the first and the last example without problems ($J/k_B = -12.1(2)$ K in **3**; $J/k_B = -1.88(1)$ K in **16**), problems arose for the Co_5 complex in **9a**. Up to approx. 100 K, a suitable model was found with $J_1/k_B = -420(5)$ K and $J_2/k_B = -150(5)$ K. At higher temperatures, the non-continuous population of higher states exceeds the limits of the available methods; accordingly, attempts to fit the thermal behavior failed. For the Mn_6 complex in **11**, suitable modeling was not possible due to the complexity of the anion. However, down to ca. 100 K, the compound follows a *Curie–Weiss* law with a *Weiss* temperature of −199 K.

3.3.3. Further properties

Several further physical properties have been investigated that allowed for a more detailed characterization of some of the compounds quoted. For instance, photoluminescence activity, vibrational excitations or thermal behavior have been explored. However, since comprehensive studies of series of related compounds are missing so far, these features are not discussed here in detail. As outlined in Section 2.2, powders of mesoporous phases have been subject matter of such investigations that are presented and discussed in the given references [23,24,38–44]. The chemical activity of A/M/14/16 phases is promising; as mentioned above (Section 3.2.2), very recent experiments have success-

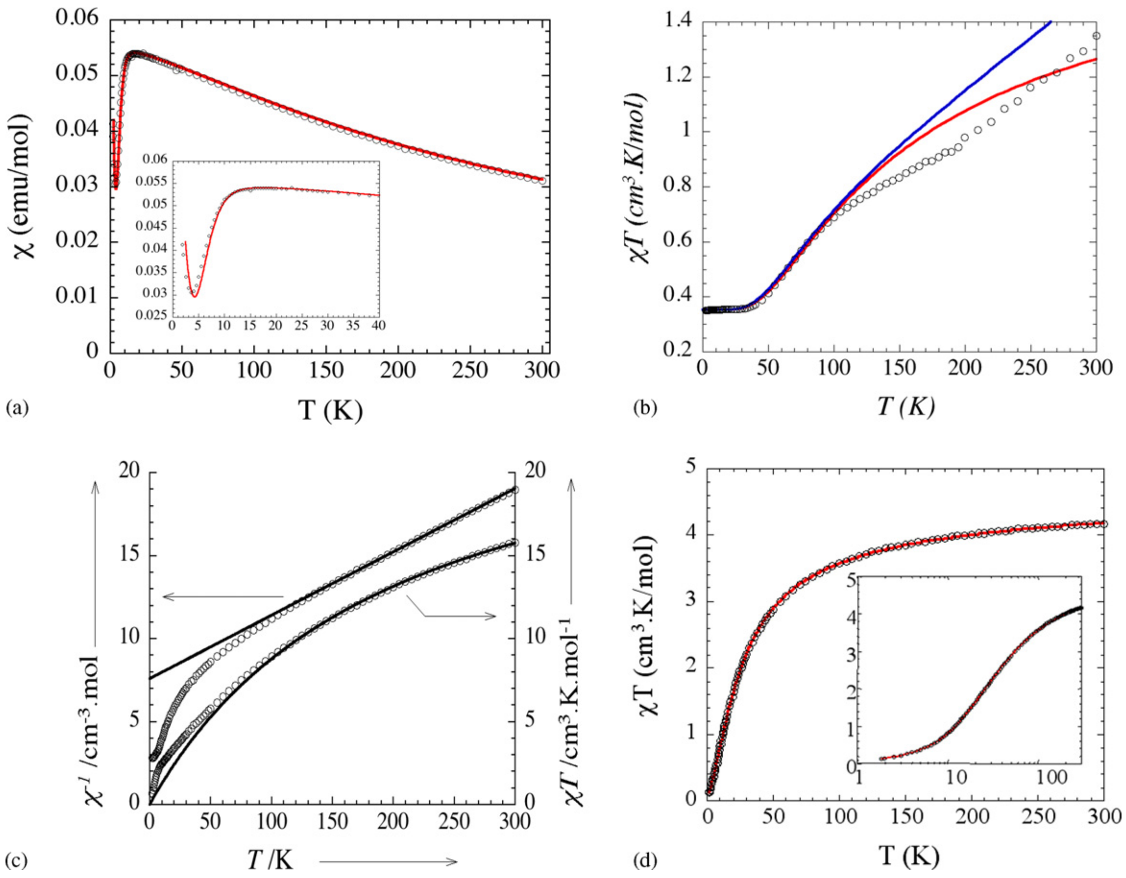

Fig. 19. $1/\chi$, χT and χ vs. T plots measured on polycrystalline samples of **6a** (a) [32], **9a** (b) [34], **11** (c) [26] or **16** (d) [35] (open circles: experimental data; solid lines: fit curves).

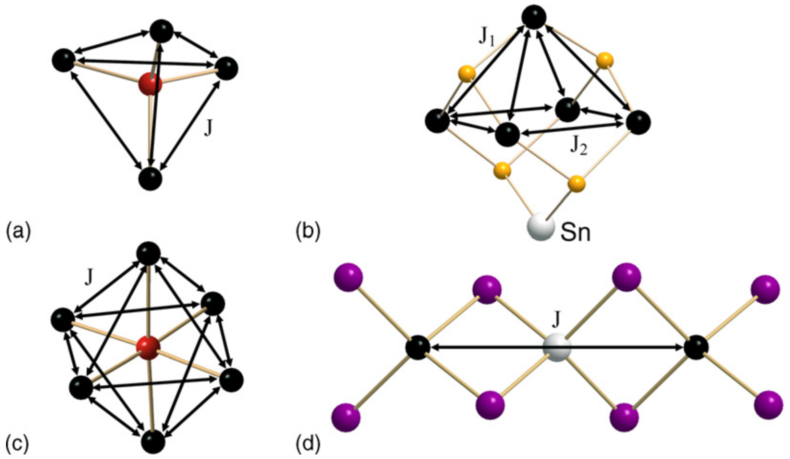

Scheme 9. Idealized exchange pathways of the magnetic coupling of four Mn^{2+} ions in **6a** (a) [32], five Co^{2+} ions in **9a** (b) [34], six Mn^{2+} ions in **11** (c) [26] or an infinite number of Mn^{2+} ions in **16** (d) [35,36].

fully proved the applicability of a Zn/Ge/S salt as photocatalyst for the H_2 formation from water [75].

4. Conclusions and outlook

In this review, a survey of compounds with ternary M/14/16 anions is provided that were synthesized by a coordination chemistry approach: by reacting alkali(ne earth) metal salts $A_4[E'E_4]$ of *ortho*-chalcogenotetrelate anions (A = Na, K, Rb, Cs, $Ba_{0.5}$; E′ = Ge, Sn; E = S, Se, Te) with transition metal compounds under ambient conditions in aqueous or MeOH solution, one gains a systematic and effective access toward a variety of different topologies of M/14/16 anions within the resulting quaternary phases, ranging from molecular complexes to one-, two- or three-dimensionally extended coordination polymers. The library of compounds obtained so far clearly shows the distinct influence of the chosen alkali(ne earth) metal counterion on the observed structural type. This permits – besides a formally coinciding composition – the formulation of a close relation to zeolite materials, which are equally formed under the template effect of the enclosed counterions. The “zeotype” properties are further underlined by some of the compounds that indeed show a nano-porous architecture. In contrast to a number of structural parallels, the opto-electronic and magnetic properties of the A/M/14/16 phases presented do not match those of zeolites; they are rather situated in the region of (wide-band) semiconductors due to the formal mixture of heavy chalcogenotetrelates and chalcogeno(transition)metallates, and they represent antiferromagnetic coupling of M centers whenever open shell metal cations are involved.

However, this very combination of zeolite-type structural and semiconductor-like electronic properties are highly attractive features of this class of compounds with regard to potential application for catalysis—suspended or even in solution, regarding the water-soluble molecular anions. At the same time this is an exciting motivation and a great challenge for future continuation of design, synthesis and characterization of A/M/14/16 phases and related compounds as an important and exciting topic of inorganic coordination chemistry.

Acknowledgements

Financial support of this work was provided by the State of Baden–Württemberg (Margarete von Wrangell fellowships for S.D., Landesgraduierten fellowship for M.M.), the Deutsche Forschungsgemeinschaft (Heisenberg fellowship for S.D.) and the Fonds der Chemischen Industrie, which we gratefully acknowledge. We are very indebted to Prof. Dr. D. Fenske, Prof. Dr. R. Ahlrichs and Prof. Dr. A.K. Powell for broad support of our research activities and provision of analytical equipment. Last but not least, we like to thank Dr. C. Zimmermann, M.K. Brandmayer, E. Ruzin, Dr. C.E. Anson, Dr. R. Clérac, Dr. F. Weigend, and Dr. O. Hampe for their valuable contributions to the present work.

References

[1] (a) B.W. Eichhorn, R.C. Haushalter, W.T. Pennington, J. Am. Chem. Soc. 110 (1988) 8704;
(b) G. Renner, P. Kirchner, G. Huttner, P. Rutsch, K. Heinze, Eur. J. Inorg. Chem. (2001) 973;
(c) J. Campbell, H.P.A. Mercier, H. Fanke, D.P. Santry, D.A. Dixon, G.J. Schrobilgen, Inorg. Chem. 41 (2002) 86.
[2] (a) M. Di Vaira, P. Stoppioni, M. Peruzzini, Polyhedron 6 (1987) 351;
(b) H.G. von Schnering, W. Hönle, Chem. Rev. 88 (1988) 243;
(c) A.J. Di Maio, A.L. Rheingold, Chem. Rev. 90 (1990) 169;
(d) R. Ahlrichs, D. Fenske, K. Fromm, H. Krautscheid, U. Krautscheid, O. Treutler, Chem. Eur. J. 2 (1996) 238;
(e) C.v. Hänisch, D. Fenske, F. Weigend, R. Ahlrichs, Chem. Eur. J. 3 (1997) 1494.
[3] (a) K.A. Hofmann, F. Höchtlen, Ber. Dtsch. Chem. Ges. 36 (1903) 3090;
(b) M. Dragnajac, T.B. Rauchfuss, Angew. Chem. 97 (1985) 745;
(b) P. Böttcher, Angew. Chem. 100 (1988) 781;
(c) M.G. Kanatzidis, S.-P. Huang, Coord. Chem. Rev. 130 (1994) 509;
(d) B.W. Eichhorn, Prog. Inorg. Chem. 42 (1994) 139;
(e) B.K. Das, M.G. Kantzidis, Polyhedron 19 (2000) 1995.
[4] Review:
M.G. Kanatzidis, A.C. Sutorik, Prog. Inorg. Chem. 43 (1995) 151.
[5] Review:
J. Wachter, Angew. Chem. 110 (1998) 782.
[6] Review:
G.W. Drake, J.W. Kolis, Coord. Chem. Rev. 137 (1994) 131.

[7] (a) D.T.T. Tran, L.M.C. Beltran, C.M. Kowalchuk, N.R. Trefiak, N.J. Taylor, J.F. Corrigan, Inorg. Chem. 41 (2002) 5693;
(b) K. Mitchell, C.L. Haynes, A.D. McFarland, R.P. Van Duyne, J.A. Ibers, Inorg. Chem. 41 (2002) 1199;
(c) D. Fenske, M. Bettenhausen, Angew. Chem. 110 (1998) 1288.

[8] (a) G. Schmid (Ed.), Clusters and Colloids—From Theories to Applications, VCH, Weinheim, 1994;
(b) S. Dehnen, A. Eichhöfer, D. Fenske, Eur. J. Inorg. Chem. (2002) 279.

[9] Review:
(a) W.S. Sheldrick, M. Wachhold, Coord. Chem. Rev. 176 (1998) 211;
(b) B. Krebs, Angew. Chem. 95 (1983) 113.

[10] (a) L. Solymar, D. Walsh, Electrical Properties of Materials, 6. Aufl., Oxford University Press, New York, 1998;
(b) A. Tanuševski, Semicond. Sci. Technol. 18 (2003) 501;
(c) C.M.I. Okoye, J. Phys.: Condens. Matter 14 (2002) 8625;
(d) F. Jellinek, in: G. Nickless (Ed.), Inorganic Sulfur Chemistry, Elsevier, Amsterdam, 1968, p. 669;
(e) F. Hulliger, Struct. Bonding 4 (1968) 83.

[11] (a) J. Gonzalez, L. Roa, R. Fouret, P. Derllez, J. Lefebvre, Y. Gunet, Phys. Stat. Sol. 225 (2001) R12;
(b) S. Siebentritt, Thin Solid Films 403–404 (2002) 1;
(c) R. Caballero, C. Guitten, Thin Solid Films 403–404 (2002) 107.

[12] K.-H. Hellwege, O. Madelung (Eds.), Landoldt-Brönstein – Zahlenwerte und Funktionen aus Naturwissenschaften und Technik, Bd. 17, Springer, Berlin, 1984.

[13] A. Lange, M.M. Kubicki, J. Wachter, M. Zabel, Inorg. Chem. 44 (2005) 7328.

[14] G.D. Albertelli, J.A. Cowen, C.N. Hoff, T.A. Kaplan, S.D. Mahanti, J.H. Liao, M.G. Kanatzidis, Phys. Rev. B 55 (1997) 11056.

[15] X. Chen, X.Y. Huang, A.H. Fu, J. Li, L.D. Zhang, H.Y. Guo, Chem. Mater. 12 (2000) 2385.

[16] B. Schiemenz, F. Ettel, G. Huttner, L. Zsolnai, J. Organometall. Chem. 458 (1993) 159.

[17] K. Merzweiler, H. Kraus, Z. Naturforsch. B: Chem. Sci. 48 (1993) 1009.

[18] (a) R.L. Bedard, S.T. Wilson, L.D. Vail, J.M. Bennett, E.M. Flanigen, in: P.A. Jacobs, R.A. van Santen (Eds.), Zeolites: Facts, Figures, Future, Proceedings of the 8th International Zeolite Conference, Elsevier, Amsterdam, 1989, p. 375;
(b) O.M. Yaghi, Z. Sun, D.A. Richardson, T.L. Groy, J. Am. Chem. Soc. 116 (1994) 807.

[19] Y. Matsuhashi, N. Tokitoh, R. Okazaki, Organometallics 13 (1994) 4387.

[20] S.S. Dhingra, R.C. Haushalter, Chem. Mater. 6 (1994) 2376.

[21] (a) C.L. Bowes, A.J. Lough, A. Malek, G.A. Ozin, S. Petrov, D. Young, Chem. Ber. 129 (1996) 283;
(b) C.L. Bowes, W.U. Huynh, S.J. Kirkby, A. Malek, G.A. Ozin, S. Petrov, M. Twardowski, D. Young, R.L. Bedard, R. Broach, Chem. Mater. 8 (1996) 2147.

[22] H. Ahari, A. Garcia, S. Kirkby, G.A. Ozin, D. Young, A.J. Lough, J. Chem. Soc. Dalton (1998) 2023.

[23] P.N. Trikalitis, T. Bakas, V. Papaefthymiou, M.G. Kanatzidis, Angew. Chem. Int. Edit. 39 (2000) 4558.

[24] P.N. Trikalitis, M.G. Kanatzidis, Mater. Res. Soc. Symp. Proc. 755 (2002) 215.

[25] (a) B. Eisenmann, H. Schäfer, H. Schrod, Z. Naturforsch. b 38 (1983) 921;
(b) K. Susa, H. Steinfink, J. Solid State Chem. 3 (1971) 75;
(c) J.-C. Jumas, E. Philippot, F. Vermont-Gaud-Daniel, M. Ribes, M. Maurin, J. Solid State Chem. 14 (1975) 319;
(d) K.O. Klepp, Z. Naturforsch. b 47 (1992) 411;
(e) K.O. Klepp, F. Fabian, Z. Kristallogr. (Suppl. 9) (1995) 189;
(f) J. Li, H.-Y. Guo, D.M. Proserpio, A. Sironi, J. Solid State Chem. 117 (1995) 247;
(g) Y. Matsushita, M.G. Kanatzidis, Z. Naturforsch. b 53 (1998) 23.

[26] M. Melullis, R. Clerac, S. Dehnen, Chem. Commun. (2005) 6008.

[27] (a) R.G. Teller, L.J. Krause, R.C. Haushalter, Inorg. Chem. 22 (1983) 1809;
(b) S. Dehnen, M.K. Brandmayer, J. Am. Chem. Soc. 125 (2003) 6618;
(c) E. Ruzin, S. Dehnen, Z. Anorg. Allg. Chem. 632 (2006) 749.

[28] (a) B. Krebs, H.J. Jacobsen, Z. Anorg. Allg. Chem. 421 (1976) 97;
(b) B. Krebs, H.-U. Hürter, Z. Anorg. Allg. Chem. 462 (1980) 143;
(c) W. Schiwy, S. Pohl, B. Krebs, Z. Anorg. Allg. Chem. 402 (1973) 77;
for recent structure elucidation of $[Na_4(H_2O)_{14}][SnS_4]$ see:
(d) R.D. Willett, A. Vij, J.M. Imhof, D.A. Cleary, J. Chem. Crystallogr. 30 (2000) 405.

[29] M. Melullis, M.K. Brandmayer, S. Dehnen, Z. Anorg. Allg. Chem. 632 (2006) 64.

[30] C. Zimmermann, M. Melullis, S. Dehnen, Angew. Chem. Int. Edit. 41 (2002) 4269.

[31] M. Melullis, C. Zimmermann, C.E. Anson, S. Dehnen, Z. Anorg. Allg. Chem. 629 (2003) 2325.

[32] M.K. Brandmayer, R. Clerac, F. Weigend, S. Dehnen, Chem. Eur. J. 10 (2004) 5147.

[33] E. Ruzin, A. Fuchs, S. Dehnen, Chem. Commun. (2006), doi:10.1039/B610833D.

[34] C. Zimmermann, C.E. Anson, F. Weigend, R. Clerac, S. Dehnen, Inorg. Chem. 44 (2005) 5686.

[35] M. Melullis, E. Ruzin, S. Dehnen, Unpublished results.

[36] C. Zimmermann, S. Dehnen, Z. Anorg. Allg. Chem. 629 (2003) 1553.

[37] (a) P.N. Trikalitis, T. Bakas, M.G. Kanatzidis, J. Am. Chem. Soc. 127 (2005) 3910;
(b) A.E. Riley, S.D. Korlann, E.K. Richman, S.H. Tolbert, Angew. Chem. Int. Edit. 45 (2006) 235;
(c) S. Haseloh, S.Y. Choi, M. Mamak, N. Coombs, S. Petrov, N. Chopra, G.A. Ozin, Chem. Commun. (2004) 1460;
(d) G.A. Ozin, E. Chomski, D. Khushalani, M.J. MacLachlan, Curr. Opin. Colloid. Interf. 3 (1998) 181.

[38] K.K. Rangan, S.J.L. Billinge, V. Petkov, J. Heising, M.G. Kanatzidis, Chem. Mater. 11 (1999) 2629.

[39] (a) M. Wachhold, K.K. Rangan, S.J.L. Billinge, V. Petkov, J. Heising, M.G. Kanatzidis, Adv. Mater. 12 (2000) 85;
(b) M. Wachhold, K.K. Rangan, M. Lei, M.F. Thorpe, S.J.L. Billinge, V. Petkov, J. Heising, M.G. Kanatzidis, J. Solid State Chem. 152 (2000) 21.

[40] M.J. MacLachlan, N. Coombs, G.A. Ozin, Nature 397 (1999) 681.

[41] P.N. Trikalitis, K.K. Rangan, M.G. Kanatzidis, J. Am. Chem. Soc. 124 (2002) 2604.

[42] P.N. Trikalitis, K.K. Rangan, T. Bakas, M.G. Kanatzidis, Nature 410 (2001) 671.

[43] K.K. Rangan, P.N. Trikalitis, C. Canlas, T. Bakas, D.P. Weliky, M.G. Kanatzidis, Nano Lett. 2 (2002) 513.

[44] A.E. Riley, S.H. Tolbert, J. Am. Chem. Soc. 125 (2003) 4551.

[45] M. Schur, H. Rijnberk, C. Nather, W. Bensch, Polyhedron 18 (1999) 101.

[46] M. Behrens, S. Scherb, C. Nather, W. Bensch, Z. Anorg. Allg. Chem. 629 (2003) 1367.

[47] J. Olkowska-Oetzel, D. Fenske, P. Scheer, A. Eichhofer, Z. Anorg. Allg. Chem. 629 (2003) 415.

[48] O. Palchik, R.G. Iyer, J.H. Liao, M.G. Kanatzidis, Inorg. Chem. 42 (2003) 5052.

[49] O. Palchik, R.G. Iyer, C.G. Canlas, D.P. Weliky, M.G. Kanatzidis, Z. Anorg. Allg. Chem. 630 (2004) 2237.

[50] P.Y. Feng, X.H. Bu, N.F. Zheng, Acc. Chem. Res. 38 (2005) 293.

[51] G.S.H.G. von Schnering, K. Peters, K.-F. Tebbe, Z. Anorg. Allg. Chem. 404 (1974) 38.

[52] I. Dance, K. Fisher, Prog. Inorg. Chem. 41 (1994) 637.

[53] (a) A. Eichhofer, D. Fenske, H. Pfistner, M. Wunder, Z. Anorg. Allg. Chem. 624 (1998) 1909;
(b) H. Pfistner, D. Fenske, Z. Anorg. Allg. Chem. 627 (2001) 575;
(c) S. Behrens, M. Bettenhausen, A. Eichhofer, D. Fenske, Angew. Chem. Int. Edit. 36 (1997) 2797;
(d) A. Aharoni, A. Eichhofer, D. Fenske, U. Banin, Opt. Mater. 24 (2003) 43.

[54] L. Eriksson, S. Frostaeng, J. Grins, Acta Crystallogr. Sect. B: Struct. Sci. 46 (1990) 736.

[55] (a) A. Eichhöfer, Eur. J. Inorg. Chem. (2005) 1245;
(b) A. Eichhöfer, P. Deglmann, Eur. J. Inorg. Chem. (2004) 349.

[56] A. Eichhofer, D. Fenske, O. Fuhr, Z. Anorg. Allg. Chem. 623 (1997) 762.

[57] (a) F. Huang, J.F. Banfield, J. Am. Chem. Soc. 127 (2005) 4523;
(b) Z.G. Ji, S.C. Zhao, C. Wang, K. Liu, Mater. Sci. Eng. B: Solid 117 (2005) 63;

(c) N.N. Kolesnikov, V.V. Kveder, R.B. James, D.N. Borisenko, M.P. Kulakov, Nucl. Instrum. Method A 527 (2004) 73;
(d) Y.L. Li, Y.H. Wang, J.F. Chen, J. Yun, J. Inorg. Mater. 18 (2003) 1362;
(e) H.Z. Zhang, J.F. Banfield, Nano Lett. 4 (2004) 713;
(f) H.Z. Zhang, B. Gilbert, F. Huang, J.F. Banfield, Nature 424 (2003) 1025.

[58] B. Krebs, H. Diercks, Z. Anorg. Allg. Chem. 518 (1984) 101.

[59] N.F. Zheng, X.H. Bu, P.Y. Feng, J. Am. Chem. Soc. 125 (2003) 1138.

[60] H.L. Li, A. Laine, M. O'Keeffe, O.M. Yaghi, Science 283 (1999) 1145.

[61] W. Schiwy, B. Krebs, Angew. Chem. 87 (1975) 451.

[62] R. Ahlrichs, N.R.M. Crawford, A. Eichhofer, D. Fenske, O. Hampe, M.M. Kappes, J. Olkowska-Oetzel, Eur. J. Inorg. Chem. (2006) 345.

[63] H.L. Li, J. Kim, T.L. Groy, M. O'Keeffe, O.M. Yaghi, J. Am. Chem. Soc. 123 (2001) 4867.

[64] A. Möller, P. Amann, V. Kataev, N. Schittner, Z. Anorg. Allg. Chem. 630 (2004) 890.

[65] X.H. Bu, N.F. Zheng, Y.Q. Li, P.Y. Feng, J. Am. Chem. Soc. 124 (2002) 12646.

[66] A.F. Holleman, E. Wiberg, N. Wiberg, Lehrbuch der anorganischen Chemie, Walter de Gruyter, Berlin, 1995.

[67] H.J. Deiseroth, K. Aleksandrov, R.K. Kremer, Z. Anorg. Allg. Chem. 631 (2005) 448.

[68] A. Lorenz, D. Fenske, Angew. Chem. Int. Ed. 40 (2001) 4402.

[69] S.T. Wilson, in: H. Robson (Ed.), Verified Syntheses of Zeolitic Materials, 2nd Rev. Ed., Elsevier, Amsterdam, 2001, p. 27.

[70] (a) J.E. Huheey, E.A. Keiter, R.L. Keiter, Anorganische Chemie: Prinzipien von Struktur und Reaktivität, 3rd ed., de Gruyter, Berlin, 2003, p. 477;
(b) A.J. Bard, R. Parsons, J. Jordan (Eds.), Standard Potentials in Aqueous Solutions, Dekker, New York, 1985.

[71] R.G. Pearson, Chemical Hardness, Wiley–VCH, 1997.

[72] X. Chen, X.Y. Huang, A.H. Fu, J. Li, L.D. Zhang, H.Y. Guo, Chem. Mater. 12 (2000) 2385.

[73] (a) C.L. Teske, Z. Anorg. Allg. Chem. 445 (1978) 193;
(b) J.H. Liao, M.G. Kanatzidis, Chem. Mater. 5 (1993) 1561;
(c) C.L. Teske, Z. Anorg. Allg. Chem. 460 (1980) 163, and literature cited therein.

[74] (a) S.S. Dhingra, D.-K. Seo, G.R. Kowach, R.K. Kremer, J.L. Shreeve-Keyer, R.C. Haushalter, M.-H. Whangbo, Angew. Chem. Int. Ed. 36 (1997) 1087;
(b) N. Pienack, W. Bensch, Z. Anorg. Allg. Chem. 632 (2006) 1733;
(c) J.B. Parise, K.M. Tan, Chem. Commun. (1996) 1687.

[75] N. Zheng, X. Bu, P. Feng, Chem. Commun. (2005) 2805.

[76] (a) N. Ding, D.Y. Chung, M.G. Kanatzidis, Chem. Commun. (2004) 1170;
(b) M. Wu, W.P. Sul, N. Jasutkar, X.Y. Huang, J. Li, Mater. Res. Bull. 40 (2005) 21.

[77] T. Okuhara, Chem. Rev. 102 (2002) 3641.

[78] (a) N. Ding, M.G. Kanatzidis, Angew. Chem. Int. Ed. 45 (2006) 1397;
(b) M.J. Manos, R.G. Iyer, E. Quarez, J.H. Liao, M.G. Kanatzidis, Angew. Chem. Int. Edit. 44 (2005) 3552.

[79] A. Loose, W.S. Sheldrick, Z. Naturforsch. B 52 (1997) 687.

[80] W.L. Masterton, D. Bolocofsky, T.P. Lee, J. Phys. Chem. 75 (1971) 2809.

[81] A.F. Holleman, E. Wiberg, N. Wiberg, Lehrbuch der anorganischen Chemie, Walter de Gruyter, Berlin, 1995, p. 1839.

[82] C.L. Cahill, J.B. Parise, Chem. Mater. 9 (1997) 807.

[83] E.K. Andersen, G. Ploug-Sorensen, Z. Kristallogr. 176 (1986) 67.

[84] R.F. Childers Jr., K.G. Vander Zyl Jr., D.A. House, R.G. Hughes, C.S. Garner, Inorg. Chem. 7 (1968) 749.

[85] P.N. Trikalitis, K.K. Rangan, T. Bakas, M.G. Kanatzidis, Nature 410 (2001) 671, Structural comparison of **5**–**7** with $(CP)_{1.6}[Hg_{1.2}SnSe_4]$, which equally comprises $[SnSe4]^{4-}$-bridged Hg atoms, is not possible due to the lack of a structural determination of this powder phase until now.

[86] N.P. Gavaleshko, M.V. Kurik, A.I. Savchuk, Sov. Phys. Semicond. 1 (1968) 920.

[87] K. Kambe, J. Phys. Soc. Jpn. 5 (1950) 48.

[88] (a) J.J. Borrás-Almenar, J.M. Clemente-Juan, E. Coronado, B.S. Tsukerblat, Inorg. Chem. 38 (1999) 6081;
(b) J.J. Borrás-Almenar, J.M. Clemente-Juan, E. Coronado, B.S. Tsukerblat, J. Comput. Chem. 22 (2001) 985.